A. Zehnacker and M. A. Suhm

DOI: 10.1002/anie.200800957

Chirality

# Chirality Recognition between Neutral Molecules in the Gas Phase

*Anne Zehnacker* and Martin A. Suhm**

**Keywords:**
ab initio calculations · chirality · hydrogen bonds · spectroscopy · supersonic expansions

*Dedicated to Professor Martin Quack on the occasion of his 60th birthday*

*Noncovalent interactions are particularly intriguing when they involve chiral molecules, because the interactions change in a subtle way upon replacing one of the partners by its mirror image. The resulting phenomena involving chirality recognition are relevant in the biosphere, in organic synthesis, and in polymer design. They may be classified according to the permanent or transient chirality of the interacting partners, leading to chirality discrimination, chirality induction, and chirality synchronization processes. For small molecules, high-level quantum chemical calculations for such processes are feasible. To provide reliable connections between theory and experiment, such phenomena are best studied in vacuum isolation at low temperature, using rotational, vibrational, electronic, and photoionization spectroscopy. We review these techniques and the results which have become available in recent years, with special emphasis on dimers of permanently chiral molecules and on the influence of conformational flexibility. Analogies between the microscopic mechanisms and macroscopic phenomena and between intra- and intermolecular cases are drawn.*

**From the Contents**



## 1. Introduction

Molecular chirality is a pervasive phenomenon in nature and has fascinated chemists and physicists alike since its discovery in the middle of the 19th century. An especially striking aspect is the homochirality of life. Macrobiomolecules tend to be homochiral, which means that they are made up from units of the same chirality. The proteinogenic amino acids all have the L configuration in human beings, while their D enantiomer is required for forming bacterial cell walls. Several hypotheses have been put forward to explain how nature has introduced such a bias favoring one enantiomer over the other.[1] Pasteur's intuition on "the dissymmetry of cosmic forces"[2] has found its fulfillment in the more modern concept of parity violation effects,[3,4] which results in a subtle difference in energy between two enantiomers of the elementary bricks of life.[5] This energy difference has been the subject of numerous theoretical calculations[6–8] but still requires experimental confirmation. Proposals and experiments based on sophisticated high-resolution spectroscopy[9,10] have not succeeded to date but have helped define the conditions for evidencing parity violation effects in chiral molecules.[11] Whether or not these effects are responsible for the homochirality of life is a completely open and difficult question to answer.

Chirality recognition, or the ability of a chiral probe to differentiate between the two enantiomers of a chiral molecule, is very important in biochemistry[12,13] and organic synthesis.[14] Most of the processes related to the interaction of a chiral ligand, such as a drug, with enzymes or protein receptors are characterized by marked enantioselectivity.[15] In particular, those underlying the sense of taste or smell[16] are often enantioselective: the two enantiomers of limonene smell different. The *S* form smells of lemon while the *R* form smells of orange. Similarly, insects, such as gypsy moths, show enantioselective sensitivity to pheromones.

Both the historic definition of chiral(ity) by Kelvin in 1893 as well as the current IUPAC definition attribute this term to a geometric property of objects.[17] Therefore, it appears slightly inconsistent to speak of chiral recognition, discrimination, induction, etc., that is, of chiral processes. The terms chirality recognition, chirality discrimination, chirality induction as short expressions for "recognition of chirality, etc." will therefore be employed herein, but we are aware that the rather unambiguous and certainly acceptable use of the adjective chiral in this context is more widespread by one to two orders of magnitude.[+]

Chirality recognition is thought to happen through the formation of weakly bound contact pairs which involve specific interactions. Among them, hydrogen bonds are of special importance. They play a major role in supramolecular chirality[18] or chirality effects in molecular imprinting.[19] Owing to their transient nature, they are difficult to identify and characterize in the condensed phase. Moreover, solvation/desolvation phenomena may affect chirality recognition processes, because the solvation energy is of the same order of

[*] A. Zehnacker
CNRS
Laboratoire de Photophysique Moléculaire, UPR3361
Univ. Paris-Sud
91405 Orsay (France)
Fax: (+33) 1-6915-6777
E-mail: anne.zehnacker-rentien@u-psud.fr
M. A. Suhm
Institut für Physikalische Chemie
Universität Göttingen
Tammannstrasse 6, 37077 Göttingen (Germany)
Fax: (+49) 551-39-3117
E-mail: msuhm@gwdg.de

[+] The distinction may become clearer if chiral/chirality is substituted for polar/polarity as another property of objects. Polarity recognition is to be preferred over polar recognition or color recognition over colored recognition.

  

magnitude as the interaction energy in these contact pairs. Although indirect information can be obtained through circular dichroism,[20] thermodynamic measurements,[21] NMR spectroscopy[22] or optical spectroscopy,[23] direct characterization at the molecular level is scarce.

Theoretical approaches to chirality recognition also are subject to severe limitations, owing to the size and the complexity of the systems at play. Numerous attempts have been made for modeling the selectivity of interactions between chiral molecules to mimic similar selectivity in enzyme–substrate systems. Empirical approaches often derive from the famous "lock-and-key" principle proposed by Fischer at the end of the 19th century to account for the specificity of enzyme reactions.[24] The "three-point rule"[25] has been applied to explain the enantiospecificity of chiral-phase chromatography.[26] Similar approaches discuss the mechanism of chirality recognition in terms of the number of interaction points or stereochemical factors.[27–30] Molecular dynamics calculations have been used to assess the role of hydrogen bonding in chirality recognition between cyclodextrins and amino acids.[22] Molecular modeling describes molecular interactions in macromolecular systems, making rational drug design possible.[31]

Information at the molecular level is highly desirable for an accurate understanding of the forces at play in chirality recognition. Gas-phase experiments on isolated neutral or ionic clusters therefore provide a powerful way of studying chirality recognition in molecular encounters, without any perturbation brought by the solvent.

*Anne Zehnacker was born in 1962, she started her studies in Strasbourg and obtained her PhD under the supervision of F. Lahmani at the Université d'Orsay. In 1991, she spent one year in the group of Ph. Millié in CEA Saclay. She is currently "Directeur de Recherche" at the French Center for Scientific Research (CNRS). Her awards include the CNRS "bronze medal" in 1992 and the prize of the Physical Chemistry division of the French Chemical Society for her work on chiral recognition. Her work focuses on molecular interactions and photo-induced processes in clusters.*

*Martin Suhm was born in 1962 and got his chemistry diploma at the University of Karlsruhe (TH) in 1985. After a year at ANU (Canberra, Australia) he moved to ETH Zürich for a PhD under the supervision of Martin Quack. In 1990, he joined David Nesbitt at the JILA (Colorado) as a postdoc before returning to the ETH for his habilitation. In 1997, he became professor of Physical Chemistry at the University of Göttingen. Awards include the medal of the ETH, the Latsis prize, the ADUC prize, and a lecturer scholarship (FCI). His research interests focus on studying intermolecular interactions by vibrational spectroscopy.*

A large body of literature has been published concerning the thermodynamics of ionic clusters of chiral molecules, using in particular, the kinetic method of Cooks et al.[32,33] Special attention has been paid to interactions involving amino acids.[34,35] Ionic clusters have been the subject of recent review articles.[36–38] Because of the large binding energy of ionic complexes, the mass spectrometry experiments are usually done at room temperature, which makes spectroscopic measurements difficult. This is the reason why direct structural information is rarely available. Vibrational spectra of protonated homochiral serine clusters have been reported recently,[39,40] in particular that of the octamer, the outstanding stability of which is proposed to play a role in the homochirality of life.[41] Several studies have described the reactivity of simple aromatic ions produced by photoionization of jet-cooled neutral complexes.[42]

In contrast to ions and zwitterions, neutral molecular complexes usually involve low binding energies. That is why their study mostly resorts to supersonic expansions, taking advantage of their capability to produce cold, weakly bound complexes in isolated conditions.

We will devote our Review to the structural, energetic, and dynamic aspects of neutral complexes, studied by electronic, vibrational, or rotational, as well as photoionization spectroscopy. These experiments focus on relatively small, tailor-made clusters, amenable to high-level quantum chemistry calculations. They enable a direct comparison between experimental data and theoretical results, providing an intimate probe of the forces at play in chirality recognition. Important molecular systems mentioned herein are depicted in Scheme 1.

The first part of this Review is devoted to chirality discrimination between molecules bearing a stereogenic center.[*] We will describe how the intermolecular forces act in a concerted way to ensure chirality discrimination. The concept of "contact points" used in empirical approaches will be replaced by more quantifiable notions. Special attention will be paid to the role of hydrogen-bonded networks and secondary interactions of electrostatic and dispersion character. The role of conformational isomerism in chirality recognition and that of interaction-induced conformational changes will also be investigated. The second part of this Review deals with the stereoselective interaction between a molecule bearing a stereogenic center and a transiently chiral or prochiral molecule. Such interactions provide mechanisms for the transmission of chirality, which is so essential in enantioselective reactions and may be termed chirality induction.[43] The last part of this Review focuses on chirality synchronization, that is, the capability of transiently chiral molecules to concertedly adjust to each other's handedness.

[*] We will denote the two enantiomers *R* and *S* using the Cahn–Ingold–Prelog nomenclature. A complex containing two *R* or *S* subunits will be called homoconfigurational or homochiral, while that containing one *R* and one *S* subunit will be called heteroconfigurational or heterochiral. Axial chirality will be classified by *P* and *M* and in mixed cases we associate *P* with *R*.

  

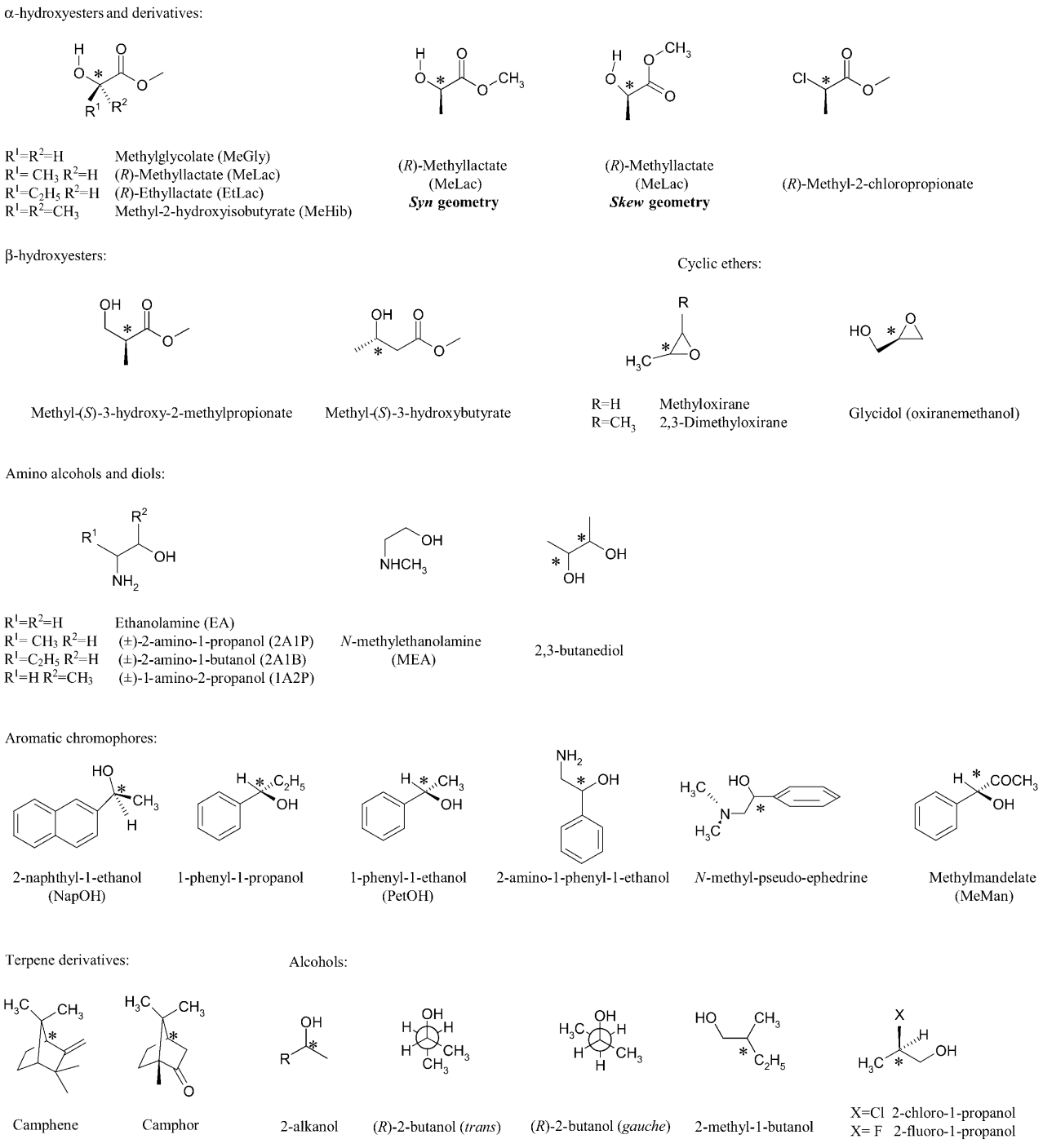


***Scheme 1.***

## 2. Experimental and Theoretical Methods

All the gas-phase experiments described herein rest on the linking of supersonic expansions with high- or medium-resolution spectroscopic techniques. This approach allows formation of non-equivalent weakly bound diastereoisomer complexes and their spectroscopic characterization (see Figure 1).

### 2.1. Supersonic Expansions

Supersonic expansion is a well established technique[44] which rests on adiabatic expansion of a gas mixture through a small-diameter nozzle. Collisions with the carrier gas cool down the internal degrees of freedom of the molecule under investigation and reduce the number of populated conformations.

  

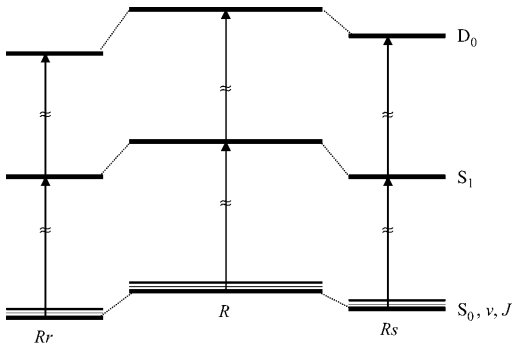


***Figure 1.*** Principle of chirality recognition in jet-cooled complexes. Complexation of a chiral selectand *R* by enantiomorphs *r* or *s* results in enantioselective shifts of the ground state ($S_0$), excited state ($S_1$), and ionic ($D_0$) energy levels leading to different spectroscopic fingerprints in rotational, vibrational, electronic, or photoionization spectroscopy.

Molecules of biological relevance show multidimensional isomerization paths leading to complex connectivity diagrams.[45–49] The conformer populations depend on their relative energy, the height of the barriers separating them, and the relaxing properties of the carrier gas. Studies of small polyatomic molecules in helium have shown that two conformers are trapped in their separate potential wells, if the potential-energy barrier isolating them is higher than about 400 $cm^{-1}$.[50,51] Traces of argon added to the helium carrier can promote collision efficiency and help to overcome somewhat larger isomerization barriers.[52] The resulting distribution of molecular or cluster conformations falls somewhere between that of the pre-expansion temperature and that of the lower rotational temperature in the jet.

As the coupling between intermolecular and intramolecular modes is usually inefficient,[53–55] formation of clusters requires three-body collisions with the carrier gas used to carry off the binding energy. There is experimental evidence that different isomers of small molecular complexes are formed in the hot early part of the expansion, and that relaxation takes place later.[51] Two mechanisms have been proposed, which can assist structural relaxation. The first one is a dissociation/recombination process.[56,57] It is put forward to explain why growth of mixed clusters shows an enrichment of the most strongly bound subunit. By analogy, it can be expected that substitution of a more stable, but less strongly bound conformer of the binding partner by a less stable but more strongly bonded one is an efficient process in complex formation. The second mechanism involves long-range interaction between the molecular complex and the polarizable carrier gas.[58] The formation of a collisional complex with the heavy carrier gas increases the internal energy, which allows the isomerization barriers to be surmounted.[59]

### 2.2. Spectroscopic Methods

The experiments described hereafter rest on the spectroscopic interrogation of the non-equivalence of diastereoisomeric complexes. The first experiments on chirality recognition in jet-cooled complexes are based on laser-induced fluorescence (LIF)[60] and resonance-enhanced two- or multiphoton ionization (REMPI).[61] These experiments require an aromatic chromophore and are based on its enantioselective stabilization (microsolvation) upon complex formation with a chiral partner, in the ground state, the excited state, and the ion as well. Combined with UV–UV double resonance (hole-burning) experiments, they give information on the number of isomers present in the expansion. The enantioselective shift of the electronic transition relative to the bare chromophore is a signature of chirality discrimination. It can be used to obtain information, though indirect, on the structure of the complexes, in particular on the role of the chromophore as a hydrogen-bond donor or acceptor,[62–65] the role of dispersion and conformation in the binding energy,[66] and the existence of OH···π interactions.[67–70]

Besides providing mass-selective electronic spectra, REMPI experiments allow measuring the binding energy of the diastereomeric complexes. Binding energy measurements rest on the two-color dissociative ionization scheme presented in Figure 2. The appearance threshold AP of the fragment

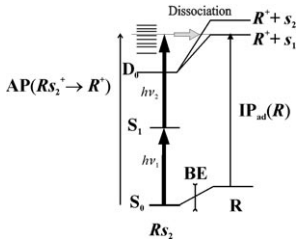


***Figure 2.*** Principle of binding-energy measurements by two-color, two-photon dissociative photoionization. The $S_0$–$S_1$ transition of one of the diasteroisomers, in this case the $Rs_2$ isomer of the *Rs* complex, is selectively excited by a first laser (frequency $\nu_1$), the intensity of which is kept as low as possible to minimize two-photon one-color ionization. The ion yield at the mass of the complex as well as the isolated chromophore is measured as a function of the energy of a second laser (frequency $\nu_2$). The binding energy (BE) of the complex is determined from the appearance threshold $AP(Rs_2^+ \rightarrow R^+)$ and the chromophore adiabatic ionization potential $IP_{ad}(R)$. Isomerization between $s_2$ and $s_1$ in the ion complicates the measurement (see text).

resulting from photodissociative ionization of the complex is related to the binding energy BE of the complex and the adiabatic ionization potential $IP_{ad}$ of the chromophore by the simple equation: $BE = AP(Rs^+ \rightarrow R^+) - IP_{ad}(R)$. Despite being conceptually simple, several difficulties pertain to this method.[71] First, it entails the knowledge of the adiabatic ionization potential of the chromophore, which can be difficult to measure if the geometry changes accompanying ionization are too large. It is therefore difficult to compare complexes with different chromophores. Similarly, if the ionization energy is large enough to allow isomerization of the solvating agent to take place in the ion, an apparent dissociation threshold is measured which is lower than the actual value (see gray arrow in Figure 2).

Vibrational spectroscopy provides information on local binding sites, in particular for hydrogen-bonded systems. Most of the effort has been focused on the region of the $\nu$(OH) and $\nu$(NH) stretch modes (3 μm). Besides its exper-

  

imental accessibility, this region is particularly sensitive to changes that result from hydrogen-bond formation. Direct absorption in a slit jet expansion by medium resolution Fourier-transform infrared (FTIR) spectroscopy[72,73] allows aliphatic systems to be studied, which are more amenable to high-level quantum chemistry calculations. Moreover, the spectra covering a wide frequency range can be recorded in one measurement. Early jet FTIR investigations of chiral clusters[74,75] used racemic mixtures only. Chirality discrimination can be detected by comparing the spectra for the racemic mixtures to the corresponding enantiopure compounds, using spectral subtraction schemes to identify heterochiral and homochiral dimers. The spectra are usually neither size nor isomer selective, although small sizes (up to tetramers) can often be discriminated by pressure dependence and isomers can often be discriminated by relaxation studies. Rigorous size-selectivity can be obtained by combining the spectra with atomic beam deflection experiments.[76]

An alternative approach is provided by IR-UV double resonance experiments.[77–83] This pump–probe method rests on the use of two lasers. The UV laser (or probe) is tuned to an electronic transition of a given species, while the IR laser (pump) is scanned in the region of interest. When the pump is in resonance with a vibrational transition of the probed species, the resulting depletion of the ground state manifests itself as a dip in the probe-induced fluorescence or ion current. Besides its sensitivity, this method has the advantage of being isomer selective as it allows the spectra of different species which absorb in the same energy range to be recorded separately. However, it is limited to complexes containing an aromatic chromophore.

Fourier transform microwave (FTMW) spectroscopy is a well-established method for obtaining the rotational spectrum of a complex, and hence its moments of inertia and global structure.[84] It has proven to be a powerful tool for distinguishing minute structural differences between conformers or diastereomers, provided that they have a sufficiently large dipole moment. It has the advantage over LIF or REMPI of being applicable to systems with no aromatic chromophore. However, it is not as sensitive as LIF or REMPI measurements, especially for species with a small dipole moment and for flexible systems. For example, only one conformer of 1-indanol has been detected by microwave experiments[85] whereas more have been seen in REMPI or LIF measurements.[86,87] Last, the microwave spectra become rapidly intractable when the size of the molecule increases, which explains that microwave spectroscopy has been limited to small systems.

### 2.3. Theoretical Approaches

As mentioned before, experimental constraints related to their vaporization and their amenability to spectroscopic investigation limit the size of the systems under study. However, they are accessible by either ab initio or density functional theory (DFT) calculations, to which we will limit ourselves herein.

Quantum chemical calculations first aim at calculating the chirodiastaltic energy, that is, the difference between the dissociation energy of the heterochiral and homochiral adducts (a negative sign of the chirodiastaltic energy means that the homochiral adduct is energetically favored over the heterochiral adduct).[88–90] In two-dimensional space (i.e. on a surface), it can be comparable to the total binding energy even for simple planar molecules,[91] whereas in three-dimensional space, it is often one order of magnitude lower than the binding energy and dictated by a subtle balance between different forces.[89] For example, it amounts to about 5% of the total binding energy in hydrogen-bonded complexes of 2-methyl oxirane and hydrogen peroxide.[89] The chirodiastaltic energy is therefore very sensitive to the method and the size of the basis set used, as well as basis set superposition error (BSSE). BSSE correction can invert its sign even at the MP2/6-311++G** level.[28] Indeed, calculations at the MP2/6-311++G(d,p) or MP2/aug-cc-pVTZ level fail to reproduce the experimental sign of the chirodiastaltic energy in methyl oxirane dimers.[92]

The second aspect of these calculations is to determine the global structure and hydrogen-bond topology of the complexes by direct comparison with the experimental spectra. It is crucial that the method used allows a complete exploration of complex potential energy surfaces (PES) of molecules with high conformational flexibility. Correlated methods are mostly applied to smaller systems such as those studied by microwave or FTIR spectroscopy,[93,94] for which the use of a large basis set is often necessary to reproduce the experimental spectra. For these small systems, a crude exploration of the surface is regularly made at the Hartree–Fock (HF) level, while a full optimization is performed with a correlated method.[95] The size of the systems containing an aromatic chromophore often precludes the use of correlated methods and they are treated at the zero-point-energy (ZPE) corrected HF or DFT level. Sometimes, the optimization step is preceded by a systematic exploration of the PES by means of a semi-empirical method.[96,97] Also, classical dynamics based on the MM3 force field have been used.[98] NBO (natural bond orbitals) analysis can be used to characterize the electron migration upon hydrogen-bond formation.[99]

For the assignment of experimental spectra to predicted conformations, spectral match and large binding energy are of prime importance. In both cases, the harmonic approximation is usually employed, because anharmonic corrections are expected to cancel out to some extent when comparing similar systems, such as in the case of chirality recognition. However, the deformation energy, that is, the energy difference between the subunits geometry within the complex and their most stable geometry as isolated entities, must also be considered.[100] This quantity is related to the kinetic aspect of complex formation: if the necessary deformation of the subunit is hindered by a sufficiently high barrier, formation of the complex may not be feasible at the low temperatures of the supersonic expansion. Fluorescence-dip IR spectroscopy shows no experimental evidence of chiral complexes with deformation energies higher than 10 $kJ\,mol^{-1}$.[69,81–83,99,101–103]

## 3. Chirality Discrimination

In this Section we describe chirality recognition between molecules carrying at least one permanent stereogenic center. Special emphasis is placed on the role of molecular flexibility in chirality recognition. "Flexibility" is the possibility for a molecule to exist in different forms of similar energy, even under the conditions of a supersonic expansion. (Conformational isomerism around simple bonds will be referred to in the following way: "g" stands for "*gauche*", when the angle between the substituents is close to 60°, and is accompanied by the subscript + or − for an angle close to 60° or −60°, respectively. "t" stands for "*trans*" (*anti*) for an angle close to 180°. Note that the enantiomer of *R*g+ is *S*g−). It is often assumed that the interaction between two chiral molecules is stereoselective provided that it involves three interaction points, one at least being stereoselective.[26,104] We first describe chirality discrimination between rigid molecules. Owing to the rigidity of their subunits, these systems involve well-defined interaction points determined by stereochemical constraints.

We then describe chirality discrimination between flexible molecules. Such molecules have several conformations which behave differently in terms of molecular interactions with a binding partner. They can adapt their structure to optimize molecular interaction (the so-called "induced fit"). This situation is true in particular for chiral selectors used in chiral-phase chromatography.[105] We describe the case of complexes of monofunctional molecules, which involve one main interaction point (hydrogen bond). Because of their flexibility, the subunits can rearrange to create secondary interaction points, such as dispersion or secondary CH···O hydrogen bonds, in addition to the major hydrogen bond interaction. Last, we present chirality discrimination effects between flexible polyfunctional molecules. Several hydrogen bonds can be formed, depending on the conformation adopted by the molecules at play.

### 3.1. Chirality Discrimination in Complexes of Rigid Molecules

#### 3.1.1. Complexes between Alcohols and Terpenes

The first examples of chirality discrimination in jet-cooled complexes rest on laser-induced fluorescence.[60,62] The fluorescent chromophore used as a discriminating agent is a naphthalene ring with a chiral side chain, 2-naphtyl-1-ethanol (NapOH). The enantioselective shift of its $S_0$–$S_1$ transition induced by complexation with a chiral molecule is the signature of the non-equivalence of the two diastereoisomer complexes.[106] In some rare cases however, the $S_0$–$S_1$ transition is located exactly at the same position (within the resolution of the laser) in the homo- and heterochiral pairs. No spectral enantiodifferentiation is obtained for complexes with terpene derivatives, such as camphene and camphor.[107,108] For both systems, the same single band is observed at low energy relative to the origin transition of the isolated chromophore. The lack of enantiodifferentiation is related to the rigidity of the molecules, resulting in a small overlap between the chiral part of the terpenic globular frame and that of the chromophore.

However, chirality-dependent fluorescence decays are observed for these complexes. The excited-state lifetimes of naphthalene derivatives are strongly sensitive to complexation, because of accidental degeneracy between the $S_1$ state and isoenergetic triplet states ($T_n$) which promotes intersystem crossing (ISC).[109,110] Complexation with camphene enantioselectively affects the resonance by shifting the energy levels and therefore considerably decreases the rate of ISC. The increased lifetimes amount to 110 and 193 ns for the homo- and heterochiral complexes, respectively, compared to 45 ns for isolated NapOH. Lengthening of the fluorescence lifetime seems to be general for 2-naphthyl-1-ethanol complexes with chiral alcohols and is enantioselective.[60,62]

The complexes with camphor show a different behavior: while the *RS* adduct $S_1$ state only lives slightly shorter than the bare molecule (42 ns), the *RR* complex exhibits a much faster decay (25 ns). This effect has been explained in terms of a singlet–singlet energy transfer between the π–π* transition of the chromophore and a close-lying n–π* transition of camphor.[111] The enantioselective fluorescence quenching of NapOH by camphor in *n*-hexane solution,[108] and concomitant camphor emission, confirms the hypothesis of an enantioselective energy transfer taking place at a rate lower than diffusion, which reproduces in an attenuated form the trend obtained in the isolated pairs in the gas phase.

#### 3.1.2. Methyl Oxirane Dimer

Propylene oxide or methyl oxirane is one of the simplest chiral molecules. Its ether ring makes it a rigid system with only one conformation.[112] Its dimer has been studied by high-resolution rotational spectroscopy combined with high-level correlated ab initio calculations.[92] Evidence was found for three homochiral and three heterochiral dimers. In all of them, the two methyl oxirane subunits are tethered through four nonconventional hydrogen bonds: the oxygen atom of each molecule acts as an acceptor for two aliphatic CH units from the other molecule. Only one homochiral dimer can be detected when neon is used as the carrier gas. The interpretation is difficult, because some stable dimers are predicted to have very weak microwave spectra. The binding energy of the observed dimers falls in the range of 15 kJ mol$^{-1}$, which is quite large for a system which only involves weak CH···O hydrogen bonds. This situation illustrates the cumulative effect of several weak interactions, which are not strong individually, but act in a concerted way to lock the complex into a stereoselective geometry.

### 3.2. The Role of Flexibility in Chirality Discrimination: Conformationally Locked versus Flexible Alcohols

#### 3.2.1. Complexes of 2-Naphthyl-1-Ethanol with 2-Chloropropan-1-ol

Strong chirality discrimination was observed in the LIF spectrum of the complex of NapOH with (*S*)2-chloropropan-

  

1-ol.[60] The interpretation of the experimental data is simplified by using a rigid solvating agent, internally bound by a weak intramolecular hydrogen bond, such as in the related 1-chloropropan-2-ol.[113] Indeed, a very simple spectrum reproducing the vibrational pattern of the chromophore is observed for the two diastereoisomeric complexes, with a red shift of $-60$ versus $-23\,cm^{-1}$ for the homo- and heterochiral pairs, respectively. The substantial chirality discrimination observed in this case is explained in terms of a strong dependence of the interaction (mainly a hydrogen bond from the chromophore to the solvent) on stereochemical factors such as steric hindrance arising from the chlorine located on the close-lying asymmetric carbon atom.

#### 3.2.2. Glycidol Dimer

A first and elementary example of chirality recognition between constitutionally identical species involves glycidol (oxiranemethanol) clusters.[114,115] Glycidol consists of a rigid oxirane ring with a methanol substituent, locked by a hydrogen bond in a double *gauche* geometry. The restricted conformational flexibility minimizes spectral congestion. Only two resulting monomer conformers, called g−g+ and g+g− hereafter, are observed by jet FTIR spectroscopy with an intensity ratio of about 4:1 (see Figure 3).

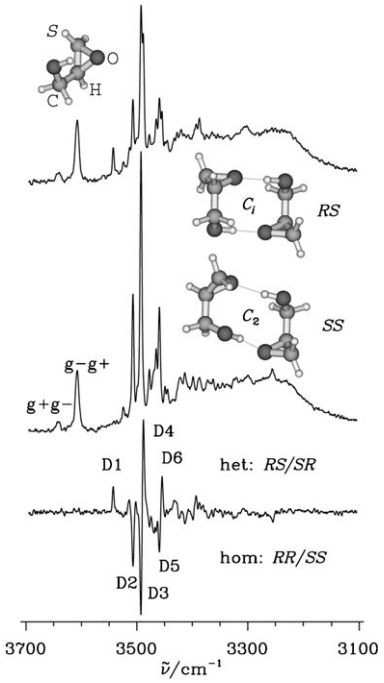


***Figure 3.*** Jet FTIR O−H stretching spectra of racemic (*RS*, top trace) and enantiopure (*S*, center trace) glycidol. From left to right, monomer, dimer, and larger cluster signals are observed. The strongest signals have a natural absorbance of less than 0.001. The bottom trace shows the spectral difference on the same scale. Negative peaks (D2, D3, D5) indicate homochiral dimers (hom: *RR*/*SS*), which dominate in the enantiopure expansion. Positive dimer peaks (D1, D4, D6) arise from heterochiral pairs (het: *RS*/*SR*), which only exist in the racemic expansion. The most stable monomer conformation ((*S*)-g−g+) and the most stable dimer structures (*RS* ($C_i$) and SS ($C_2$), activated addition type) are shown (adapted from ref. [114]).

Despite the restricted monomer flexibility, the dimer spectra observed in the OH stretch region are surprisingly crowded (see Figure 3). Their discriminated fraction (that is, their chirality dependent fraction) consists of three bands for each diastereoisomer. Only the strongest one of each survives in an argon expansion, suggesting that it corresponds to the most stable homo- or heterochiral dimer. On the basis of HF, B3LYP. and MP2 calculations, they have been assigned to head-to-tail structures in which the methanol part of each g−g+ subunit interacts with the oxirane oxygen atom of the other subunit. The resulting eight-membered ring (counting only heavy atoms) with two OH···O interactions is called $C_8$ hereafter (Figure 3). The spectral difference between the homo- (D3) and heterochiral (D4) dimers is small. Note that in this case, the terms homo- and heterochiral fulfill the original, narrow definition given by Kelvin.[116] Some of the weaker OH bands differ by as much as $19\,cm^{-1}$. They may involve five-membered rings ($C_5$) in which the methanol subunit inserts within the intramolecular hydrogen bond of the other one. These compact structures react more sensitively to chirality differences than the open $C_8$ structures, both in terms of binding energy and vibrational frequencies. This insertion motif will be encountered several times in later Sections.

#### 3.2.3. 2-Butanol Dimer

Increased flexibility results in a more complicated spectroscopic signature. The flexible (±)-2-butanol can adopt at least three conformations, one *trans* (t) and two *gauche* (g+ and g−),[117] resulting in at least nine geometries of the dimer. Only the most stable heterochiral dimer has been fully characterized by rotational spectroscopy.[95] It shows both a large a-transition dipole and a quite distinctive pattern owing to a small B−C value, which helps in the assignment. No assignment was obtained for the homochiral dimer, despite its large transition moment, which tends to confirm its predicted lower stability. The complexity of the system is increased by the fact that the two flexible subunits mainly interact through a single hydrogen bond. In line with this situation, the jet FTIR spectrum of 2-butanol dimer shows little chirality discrimination in the OH stretching region.[118] Dispersion is of reduced importance in small aliphatic systems. In contrast, it plays an important role in aromatic molecules with larger polarizability, where it provides additional anchoring points.

#### 3.2.4. 2-Naphthyl-1-Ethanol Complexes with Secondary Alcohols

The importance of dispersive interactions is illustrated by the example of chirality discrimination between NapOH and secondary aliphatic alcohols with a carbon chain ranging from $n=3$ (2-butanol) to $n=8$ (2-octanol).[62,66] The LIF spectra of all complexes (see Figure 4) share common trends. The transition origin is always shifted down in energy relative to the isolated chromophore, indicating that the chromophore acts as the hydrogen-bond donor. UV-UV hole burning experiments indicate that there are two different isomers for each diastereoisomer. The first one, called F hereafter, displays the most red-shifted transition, accompanied by a

  

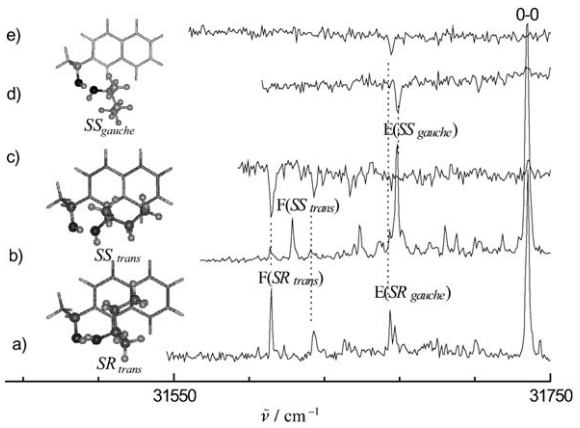


***Figure 4.*** Fluorescence excitation spectrum of the $S_0$–$S_1$ transition of the complexes between (*S*)-NapOH and a) (*R*)-2-butanol b) (*S*)-2-butanol. The transition origin of isolated NapOH is denoted by 0-0, that of the homochiral complexes by *SS* and that of the heterochiral by *SR*; *trans* and *gauche* stand for the conformer of 2-butanol contained in the complex, E and F stand for extended and folded shape of the complex, respectively (see text for details). UV-UV double resonance spectrum with the probe laser set on the bands denoted by the vertical dashed lines for c) $SR_{trans}$ d) $SS_{gauche}$ e) $SR_{gauche}$. The most stable calculated complexes of the homochiral and heterochiral complexes with the two major conformers of 2-butanol are shown.

low-frequency progression, with a red shift systematically larger for the heterochiral than the homochiral adduct. The $S_0$–$S_1$ spectrum of the second isomer, called E hereafter, shows a single feature which happens at slightly different energy for the two diastereoisomers. Theoretical calculations assign the F and E features to complexes involving different conformers of the secondary alcohol, discussed herein using the example of 2-butanol.[66] The F band is assigned to a complex with a hydrogen bond from NapOH to the *trans* form of 2-butanol, which was later characterized by jet rotational spectroscopy.[117] In this complex, the alkyl chain of 2-butanol is folded over the aromatic frame, which results in dispersion interactions, hence a red-shifted transition. The red shift is systematically larger in the heterochiral complex (147 vs. 125 cm$^{-1}$), because of a more-folded geometry resulting in more dispersion than in the homochiral adduct. The *gauche* isomer of 2-butanol forms extended complexes with less dispersion interaction and hence reduced red shift of the $S_0$–$S_1$ transition (73 and 69 cm$^{-1}$ for the hetero- and homochiral complex, respectively). The limited interaction between the aromatic ring and the solvent makes the *gauche* structure much less sensitive to chirality discrimination than the one involving the *trans* form. The difference in the diastereoisomer transition energy is only 4 cm$^{-1}$ when the complex contains the *gauche* form while it amounts to 22 cm$^{-1}$ for the *trans* form. The size of the red shift, which reflects changes in dispersion brought by electronic excitation, is seen to correlate with the extent of chirality discrimination. The dependence of the red shift on solvent configuration has also been discussed for complexes between 1-phenyl-1-propanol and secondary alcohols.[119] Moreover, the red-shift observed in this case is smaller than expected from the proton affinity of the complexing agent, in contrast to primary alcohols.[42] This result confirms that the electrostatic interaction is not the only force at play in these systems.

These results emphasize the role of dispersion forces in chirality recognition. Superimposed on the main intermolecular force (a single hydrogen bond), dispersion provides secondary interactions which are in turn responsible for chirality recognition. This observation parallels the one of Craig and Mellor.[88] The intermolecular forces responsible for host–guest binding (in this case, the hydrogen bond) are not the same as those causing chirality recognition (in this case, dispersion). As the *gauche* conformers of alcohols are less prone to form folded complexes involving large dispersion, hence secondary interactions, they are less articulate in terms of chirality discrimination.

### 3.3. Flexibility and Energetic Aspects of Chirality Discrimination

Binding-energy measurements have been pioneered by Latini et al. on the 1-phenyl-1-propanol complexes[98,120] which are more suitable than naphthalene derivatives for one-color two-photon ionization. Three different conformers of 1-phenyl-1-propanol have been supposed to co-exist in the supersonic expansion, these conformers involve rotation around the C–O bond. The $S_0$–$S_1$ spectra of the homochiral and heterochiral complexes with 2-butanol are characterized by two single, intense bands. These spectra seem to indicate that only two out of the three isomers of 1-phenyl-1-propanol form complexes with 2-butanol. Binding-energy measurements have been performed for the complexes responsible for the most red-shifted band. The homochiral complex is stabilized relative to the heterochiral adduct by $4.6 \pm 1.7$ kJ mol$^{-1}$ in the ground state.

Similar measurements have been made on the simpler 1-phenyl-ethanol (PetOH), which only has one isomer under jet-cooled conditions.[68] UV-UV hole-burning experiments have demonstrated the co-existence of two kinds of PetOH:2-butanol complexes (see Figure 5). Complexes of the first type are built from the *trans* form of 2-butanol and are called $Rs_1$ and $Rr_1$. They show a large red-shift of their electronic transition, which is larger for the heterochiral (132 cm$^{-1}$) than for the homochiral adduct (121 cm$^{-1}$) and similar to those observed in the NapOH complexes. The second type with the *gauche* form of 2-butanol manifests itself by a single weak line at $-101$ cm$^{-1}$ in the *Rs* complex, and is called $Rs_2$ hereafter. A similar complex probably exists for *Rr*, but the band observed in this region was too weak to be probed. The binding energies of the $Rs_1$ and $Rs_2$ complexes differ by 3.3 kJ mol$^{-1}$ which corresponds, within the error, to the calculated energy difference between the *gauche* and *trans* forms of 2-butanol.[66,117] The binding energy of the $Rr_1$ and $Rs_1$ complexes can also be compared, because they contain the same conformer of the solvent. The chirodiastaltic energy is $-2.9$ kJ mol$^{-1}$, similar to the related phenyl-1-propanol complex.

Phenyl-1-propanol:2-pentanol complexes show a surprising behavior. While both the spectroscopic fingerprint and the binding energy of the *Rr* complex resemble that of the *trans* 2-butanol complex, the *Rs* complex shows a dense bunch of

  

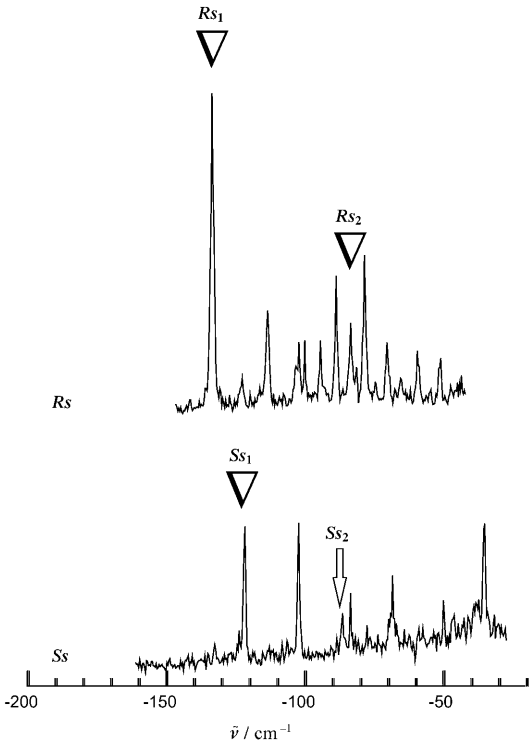


***Figure 5.*** Mass-resolved $S_0$–$S_1$ excitation spectrum of the PetOH:2-butanol homochiral (bottom) and heterochiral (top) complexes. The zero of the energy scale is taken at the isolated PetOH chromophore origin. The bands denoted by ▽ have been probed by UV-UV hole burning spectroscopy and shown to correspond to different isomers of the complex (see text for details).

blue-shifted bands and a much lower binding energy. This feature indicates that the two diastereoisomers may not contain the same conformer of 2-pentanol.[98,120]

### 3.4. Competition between Inter- and Intramolecular Interactions: Cooperative Effects

We have seen that *gauche–trans* isomerism in alcohols results in subtle differences in dispersion energy, which have consequences for the binding energy of the complexes and for the extent of chirality discrimination. More important effects are observed when the subunits at stake are bifunctional compounds showing an intramolecular hydrogen bond. Their conformers can be classified in terms of "closed" and "open" conformations, respectively, depending upon whether or not the hydrogen bond is formed. The energy difference between the isomers at play is much larger than that involved in *gauche–trans* isomerism in alcohols. On the other hand, the closed and open conformers may have different binding properties to the selectand.

#### 3.4.1. Complexes between Diols and Alcohols

Butane-2,3-diol is a case of intramolecular chirality discrimination.[121] The two chirality centers are not only linked by a hydrogen bond, but also by a chemical bond. As a result, there are large differences between the homochiral and heterochiral (*meso*) forms in what is better known as conventional diastereoisomerism. In terms of intermolecular diastereoisomerism, complexation of diols by (*R*)-(+)-1-phenyl-1-propanol has been studied by resonant two-photon ionization (R2PI) combined with molecular-dynamics calculations.[122] The major characteristic of these complexes is a smaller red-shift of the electronic transition in the complex with the diol relative to the corresponding monofunctional alcohol. This observation is rationalized in terms of a secondary OH···π interaction which decreases the electrostatic forces in the $S_1$ state relative to the $S_0$ state. This reasoning is based on the premise that the nature of the primary interaction and the geometry of the subunits are the same in the two complexes to be compared.

Counterexamples are however frequent: heterochiral complexes of 2-methyl-1-butanol and 2-amino-1-butanol both involve a OH···O hydrogen bond as the main interaction, and show exactly the same red-shift ($-84\ cm^{-1}$)[66,101] despite 2-amino-1-butanol being a bifunctional compound. Moreover, complexes with similar shifts of their electronic transition can involve totally different interactions: heterochiral and homochiral complexes of NapOH and 1-amino-2-propanol have completely different structures (OH···O vs. OH···N hydrogen bond), even though the shift of their electronic transition is similar ($-90$ vs. $-110\ cm^{-1}$). Therefore IR spectroscopy is necessary to understand the interactions in bifunctional compounds.

#### 3.4.2. IR Spectroscopy of Complexes between Ethanolamine Derivatives and Alcohols

Ethanolamine derivatives adopt different geometries depending on the surroundings.[123–127] Under isolated conditions, their most stable structure, called "closed form" hereafter, displays an internal hydrogen bond with the OH group acting as the proton donor to the amino group. In supersonic expansions, there is no evidence for a less-stable alternative conformer.[125,127–130] However, the conformational preference of ethanolamine derivatives is profoundly modified by the surrounding. A so called "open form" involving a free OH group and a NH···O interaction is detected in solution and in the neat liquid, where the involvement of the molecule in intermolecular hydrogen bonds results in a competition between inter- and intramolecular OH···N interactions.[123,124]

This competition also exists in jet-cooled complexes and depends on chirality. A series of complexes between NapOH and chiral or non-chiral amino alcohols has been studied by LIF and double resonance UV-UV or IR-UV spectroscopy.[99,101,102] Extensive theoretical work has also been performed, which combines a semi-empirical method, DFT calculations, and NBO analysis performed on MP2 single points. The obtained structures will be described for the example of the NapOH:1-amino-2-propanol (1A2P) complexes.

The three most stable calculated forms of the homochiral complex are shown in Figure 6. Two of them are built from the closed form of 1A2P and are almost isoenergetic. Their

  

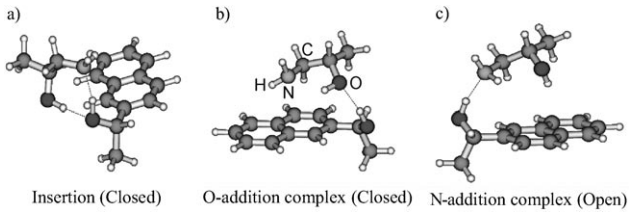


***Figure 6.*** The most stable complexes calculated for NapOH:1A2P *SS* complexes a) insertion (BE including BSSE correction = 18.8 kJ mol$^{-1}$), b) O-addition (BE = 18.8 kJ mol$^{-1}$), c) activated N-addition (BE = 25.1 kJ mol$^{-1}$). The nature of the conformer of 1A2P (open or closed) contained in the complex is given in parentheses.

binding energy including ZPE and BSSE correction amounts to 18.8 kJ mol$^{-1}$. The first one, called hereafter "insertion complex", involves insertion of the hydroxy group of NapOH within the intramolecular hydrogen bond of 1A2P (Figure 6a). The opening of the intramolecular bond results in a large deformation energy of 1A2P (12.6 kJ mol$^{-1}$). The second one, referred to as the "O-addition" complex, involves an intermolecular hydrogen bond from the NapOH hydroxy group to that of 1A2P (Figure 6b). The quasi-retention of the 1A2P molecular structure manifests itself by a very small deformation energy (less than 2.1 kJ mol$^{-1}$). The last calculated complex, the "N-addition complex", is built from the open form of 1A2P (Figure 6c). It involves addition of the NapOH hydroxy onto the amino group of 1A2P; a secondary OH···π interaction reinforces the cohesion of the complex.

Ethanolamine derivatives behave systematically: an O-addition structure is observed for all the complexes with NapOH. For chiral derivatives, it is observed for both enantiomers. Its electronic transition corresponds to the less-shifted band in the LIF spectrum (shifted by less than 90 cm$^{-1}$), shown in Figure 7, and is always lower in energy in the heterochiral than in the homochiral adduct. Its IR spectrum is typical of OH groups involved in OH···O interactions. In some cases, (ethanolamine, N-methyl ethanolamine, the homochiral complex with 1A2P or 2-amino-1-propanol (2A1P)), an additional band is observed at ($-100 \pm 10$) cm$^{-1}$ from the isolated chromophore origin. This band is assigned to an "N-addition" complex on the basis of its vibrational spectrum. It is worth noting that this band always appears in the same energy range and that it is only observed in homochiral systems.

All these complexes are bound by hydrogen-bonded networks involving cooperative effects. For example, the 1A2P $\nu$(OH) stretch mode frequency is lower in the O-addition complex (below 3470 cm$^{-1}$) than in the isolated molecule (3556 cm$^{-1}$): the fact that the hydroxy group of 1A2P is involved as a hydrogen-bond acceptor makes it a better donor, which reinforces the intramolecular hydrogen bond.

Surprisingly, insertion complexes are never detected experimentally. This behavior has been explained in terms of reorganization energy. It contrasts with the hydrate of 2-amino-1-phenylethanol, which shows disruption of the intramolecular hydrogen bond to allow for insertion of water.[131] Indeed, insertion of the bulky NapOH chromophore is much more demanding in terms of the reorganization barrier than that of water and it is certainly not assisted by quantum tunneling.

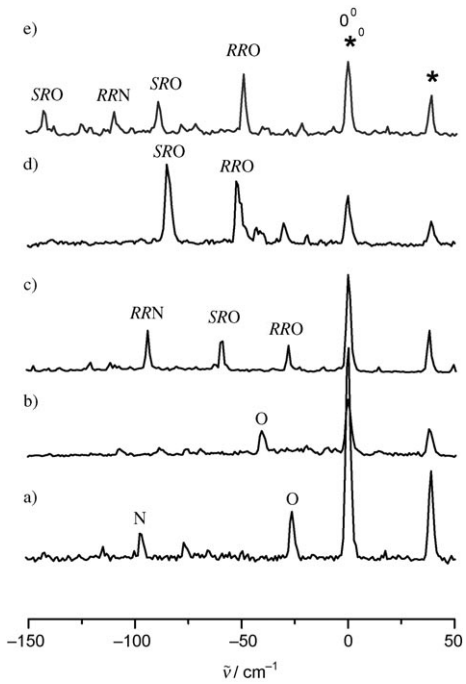


***Figure 7.*** Fluorescence excitation spectrum of the $S_0$–$S_1$ transition of the complexes between NapOH and a) ethanolamine b) *N*,*N*-dimethylethanolamine c) 2-amino-1-propanol, d) 2-amino-1-butanol, e) 1-amino-2-propanol. The transitions arising from isolated NapOH are denoted by *, those from the homochiral complex by *RR* and the heterochiral complexes by *SR*. O and N stand for O-addition and N-addition complexes, respectively.

The second surprising observation is the elusiveness of heterochiral N-adducts in 1A2P and 2A1P. Their absence cannot be explained by energetics, as the calculated binding energy of both diastereoisomers is of the same order (26.7 vs. 25.1 kJ mol$^{-1}$ for the ZPE and BSSE corrected binding energies of the heterochiral and homochiral complexes of 1A2P, respectively). The explanation probably stems from kinetic factors and subtle differences in interaction energies on the formation path towards the hetero- and homochiral complex. This behavior is reminiscent of enzymatic catalysis, where the enzyme binds transition states and reactive intermediates in preference to reactants,[132] and in particular asymmetric catalysis by hydrogen-bond formation between the reactant and the chiral catalyst.[133]

Last, these systems provide an illustration of the subtle structural parameters accessible by IR spectroscopy. In the case of 2-amino-1-butanol, a single O-addition complex is observed for both *RR* and *SS* adducts. Their structures are very similar to each other, as are their binding energies. However, they slightly differ by the linearity of the intermolecular OH···O hydrogen bond (175° for *RS*, 170° for *SS*), which in turn results in a larger electron-density transfer to the antibonding σ*(OH) orbital localized on the O–H bond of NapOH. The experimentally observed $\nu$(OH) stretch frequency is therefore about 20 cm$^{-1}$ lower in *RS* than in *RR*.

  

### 3.4.3. *IR Spectroscopy of Lactic Acid Derivative Clusters*

α-Hydroxyesters have a hydroxy substituent in the position α to the ester group, directly at the chiral center (see Scheme 1). Their most stable *syn* form involves an intramolecular hydrogen bond from the O–H to the C=O of the ester. Less stable *skew* forms involving an $OH\cdots OCH_3$ contact have been calculated to be $9\,kJ\,mol^{-1}$ higher in energy. In contrast with ethanolamine, both isomers involve an intramolecular hydrogen bond and are therefore of the "closed" type. However, the hydrogen bond involved in the *syn* form is much stronger than that involved in the *skew* form. Despite being observed in matrix isolation experiments,[134] the *skew* isomer of methyl lactate was detected neither in microwave measurements[135] nor in FTIR spectroscopy of jet-cooled species.[93,136]

As for the ethanolamine complexes, the structures of α-hydroxyester dimers calculated at the B3LYP or MP2 level consist of addition or insertion complexes. Contrary to ethanolamine complexes, addition complexes involving two α-hydroxyester molecules also require opening the intramolecular hydrogen bond of one or both of the subunits so that the OH group can interact with the other molecule. In contrast to the O-addition in ethanolamine, we therefore call them "activated addition complexes". If both intramolecular hydrogen bonds open up, a head-to-tail activated addition structure ($C_8$, as in the glycidol case shown in Figure 3) is obtained. In the $C_5$ dimer, the hydroxy group of one of the subunits inserts into the intramolecular hydrogen bond of the other one (as in Figure 6a).

Clusters of methyl lactate (MeLac), ethyl lactate (EtLac), as well as their nonchiral analogues methyl glycolate (MeGly) and methyl hydroxyisobutyrate (MeHib), have been studied by FTIR absorption in a slit jet.[93,136] The IR spectra of the MeLac clusters are presented in Figure 8. Comparison with size-selected experiments based on atomic beam deflection and depletion spectroscopy has confirmed the assignment of the least red-shifted cluster bands to dimers.[76,137] The dominant homochiral band was shown to belong to a $C_2$-symmetric dimer ($C_8$ structure) with OH···O=C hydrogen bonds, this conclusion was based on the weak exciton coupling evident in the Raman spectrum,[138] comparison with MeGly and MeHib,[93] the C=O red-shift, and on argon coating studies.[136] The heterochiral dimer appears to absorb at slightly higher wavenumber, indicative of some chirality recognition. Weak satellite bands complicate the interpretation. They could either be due to less stable isomers or to combination transitions involving low-frequency vibrations.

The influence of adding an aromatic ring to the same hydrogen-bond motif has been studied by replacing one MeLac monomer by its aromatic analogue, methyl mandelate (MeMan see Scheme 1). The MeMan:MeLac or MeMan:MeGly dimers have been studied by LIF and fluorescence-dip IR spectroscopy.[100] Their behavior clearly differs from that of MeLac aggregates. The single absorption band as observed in the $S_0$–$S_1$ spectrum rules out the presence of more than one isomer in the conditions of a pulsed pinhole jet. This band is slightly shifted to the blue of the bare molecule origin and appears at almost the same position for the complex of (*R*)-MeMan with MeGly and (*R*)- or (*S*)-MeLac, indicating a significant structural similarity between them. Its IR spectrum exhibits a doublet, characteristic of a $C_5$ complex, located at 3501 and 3535 $cm^{-1}$. Taking into account both binding and reorganization energy, and the correspondence between the experimental and calculated frequencies, it has been concluded that the complexes detected are built upon the less stable *skew* form of MeLac. This metastable *skew* form may temporarily exist in the collision zone of the expansion and then relax towards a more stable form.[103] Although they are not detected in the cold zone, higher energy conformers can play a role in complex formation[70,101] because their structure suits that of its partner better.

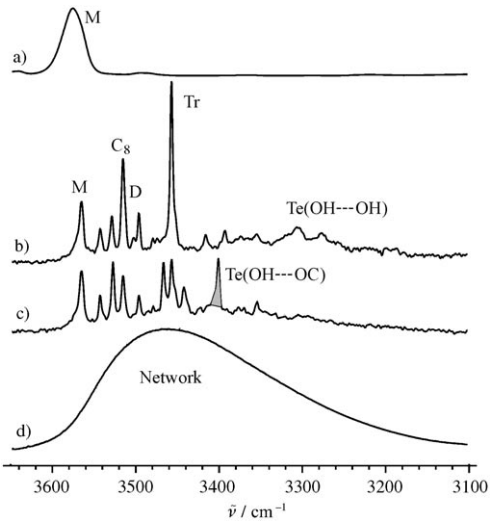


***Figure 8.*** Jet FTIR O–H stretching absorbance spectra of expansions of enantiopure and racemic methyl lactate seeded in helium, compared to stationary gas- and liquid-phase spectra. a) room-temperature gas phase, showing only monomer signals (M), b) expansion of enantiopure methyl lactate, showing signals from cold monomers (M), dimers (D), a single trimer band arising from a $C_3$-symmetric cluster (Tr), and mostly OH···OH connected tetramers (Te), c) expansion of racemic methyl lactate, showing the same M, but different D, Tr, and Te bands, the Te bands arise from OH···OC hydrogen bonds and are therefore significantly shifted from the homochiral Te signals (see gray shading and next Figure 9), d) room-temperature liquid phase, showing the broad distribution of hydrogen-bond shifts in the extended network, which is unresolved and does not differ appreciably between enantiopure and racemic samples as a result of thermal excitation.

More efficient complex formation from a minor-abundance conformer has also been supposed for (±)-1-phenyl-1-propanol complexes with chiral secondary alcohols or (±)-3-hydroxytetrahydrofuran. The relative intensity of the bands assigned to (±)-3-hydroxytetrahydrofuran complexes containing the three isomers of (±)-1-phenyl-1-propanol is modified relative to the isolated molecule.[98] In the case of bidentate molecules, such as α-hydroxymethylesters, only one or two out of the three conformers of (±)-1-phenyl-1-propanol predominate in the complex.[65] Similarly, complexation efficiency for the two isomers of 1-indanol depends on chirality.[87]

More pronounced chirality discrimination effects were found in trimers (Tr) and tetramers (Te) of methyl lactate (see

Figure 8). Investigation of the C=O stretching spectrum[136] and of the Raman jet spectrum[138] clearly shows that O–H···O=C hydrogen bonds are given up in favor of alcohol-like cooperative O–H···O–H···O–H ring topologies. In the trimer built from three molecules of the same handedness, this leads to a bowl-shaped $C_3$-symmetric structure with secondary C–H···O=C contacts. Its IR spectrum is dominated by the degenerate O–H stretching vibration, whereas the Raman spectrum has more intensity in the totally symmetric vibration. The large splitting between these two transitions demonstrates the O–H···O–H character,[138] as does the blue-shifted C=O stretching fundamental. Trimers built from molecules of mixed chirality are less symmetric and give rise to more complex spectra. The tetramers feature the same O–H···O–H connectivity, profiting from a cooperative enhancement which the O–H···O=C contact cannot offer. There is one exception: The tetramer built from two *R* and two *S* units in an alternating *RSRS* sequence, switches back to the O–H···O=C connectivity, giving rise to a characteristic IR band.[139] This change is due to a particularly compact $S_4$-symmetric structure (Figure 9), which offers a maximum of attractive secondary interactions. To build the structure, the internally hydrogen-bonded OH group in neighboring *syn* lactate units has to be distorted in alternating directions (*r*/*s*) and this alternation has to match the alternation of the lactate configuration (*R*/*S*). Each mismatch between the two alternations is equivalent to an energy penalty of several kJ mol$^{-1}$, making the *RRRR*, *RRRS*, and *RRSS* variants much less stable. Dissociation of the achiral lactate tetramer into a homochiral pair of *RS* dimers may be considered as an example for "la coupe du roi" (for an explanation and an example of "la coupe du roi", see Ref. [140]). The cut between the two halves includes the $S_4$ axis to conserve the integrity of the lactate units. The resulting dimers are initially homochiral, but they can rearrange by closing the second hydrogen bond to form stable achiral or chiral structures.

It is remarkable that the chirality-induced hydrogen-bond topology switch in lactate tetramers is not predicted by density functional theory, presumably owing to missing long-range dispersion.[141] However, the effect is very pronounced at the MP2 level.[139] The structure loses its competitiveness by replacing the $C_\alpha$–H atom with a methyl group, whereas it can also be realized in MGly tetramer.[93] Interestingly, the crystal structures of enantiopure and racemic serine also differ in the type of hydrogen bonding, O–H···O–H versus O–H···O=C. Like racemic lactate tetramers, racemic serine can form O–H···O=C links.[142]

#### 3.4.4. IR Spectroscopy of Complexes between Lactic Acid Derivatives and Alcohols or Amino Alcohols

The double resonance technique has been applied to the study of 1:1 and 1:2 clusters of NapOH with α-hydroxyesters.[143] The LIF spectra obtained by mixing (*R*)-NapOH with MeGly, MeHib, and the two enantiomers of (±)-MeLac and (±)-EtLac are shown in Figure 10. Based on the spectra the complexes can be separated in two classes. The first is characteristic of MeGly and the heterochiral complexes of MeLac and EtLac and is called **IA** hereafter. It shows a strongly red-shifted progression, assigned to a 1:1 complex, and built on a 20 cm$^{-1}$ mode assigned to a low-frequency motion of the ester group. A second 1:1 complex, denoted **IB**, manifests itself by a strong isolated band slightly shifted to the blue relative to the isolated chromophore.

The homochiral mixtures behave completely differently. Strong bands assigned to 1:2 complexes are experimentally

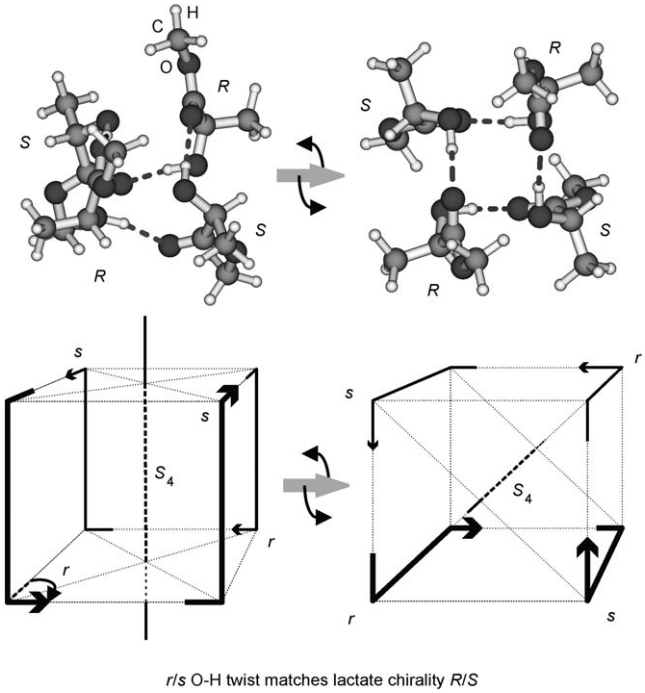


***Figure 9.*** $S_4$-symmetric methyl lactate tetramer structure involving alternating configurations of the monomer units, viewed from different angles (from left to right: tilting of the symmetry axis towards the observer by about 90°), and corresponding projections of the hydrogen-bond topology on a cube. *s*/*r* stands for the OH twist direction from the *syn* monomer structure to the monomer conformation in the tetramer.

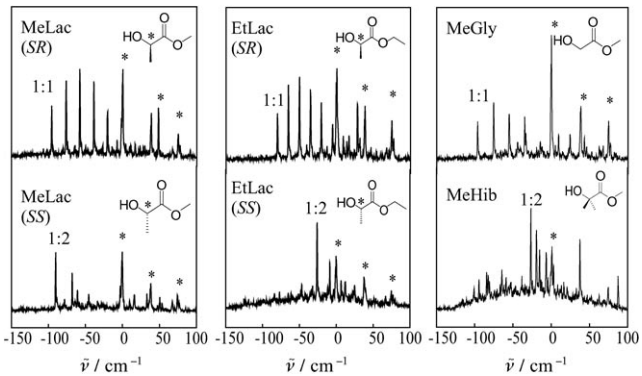


***Figure 10.*** Fluorescence excitation spectrum of the $S_0$–$S_1$ transition of the complexes between (*S*)-NapOH and α-hydroxy esters. The zero of the energy scale is taken at the origin of the isolated NapOH chromophore. The transition origin of isolated NapOH is denoted by *, that of the homochiral complexes by *RR* and of the heterochiral by *SR*. The complexes containing one NapOH and one or two α-hydroxy ester molecules are denoted by 1:1 and 1:2, respectively.

  

observed but 1:1 complexes, if any, are hardly detected in the LIF spectrum. Whatever the experimental conditions, it is clear that no **IA** complex is observed.

The IR spectra of the heterochiral complexes **IA** and **IB** of NapOH:MeLac are both characteristic of addition complexes from the interaction of the NapOH hydroxy group with MeLac in its *syn* form (see Figure 11). The frequencies observed in the spectra of the complexes are both red shifted relative to their counterpart in the isolated molecules NapOH and MeLac, because of cooperative effects, which reinforce the intramolecular hydrogen bond.

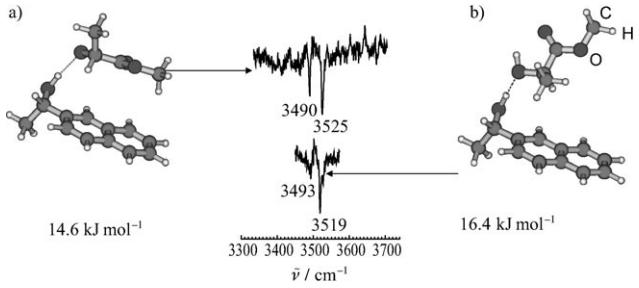


***Figure 11.*** Experimental double resonance spectrum as well as calculated structures of a) **IA** heterochiral complex, b) **IB** heterochiral complex.

Despite the similarity between their IR spectra, the assignment of **IA** and **IB** to calculated structures was made possible by considering the shift of their electronic transition. The red shift observed for **IA** corresponds to an increase of dispersion upon electronic excitation. It has been attributed to the folded structure shown in Figure 11 a. Conversely, the complex shown in Figure 11 b involves less dispersion and has been assigned to the **IB** structure with a blue-shifted electronic transition.

The missing **IA** type complex in the homochiral adduct of MeLac or EtLac, as well as in MeHib, has been related to the presence and the stereochemistry of the hydrogen atom in the α position of the ester. In the calculated **IA** structure of NapOH:MeLac, the hydrogen atom on $C_\alpha$ is directed towards the naphthalene ring while the methyl group is pointing outwards. This geometry cannot be obtained in the homochiral complex or in that with MeHib, because of steric hindrance brought by the methyl group. The same behavior is observed for β-hydroxyesters where no fluorescent 1:1 complex is observed for one of the diastereoisomer complexes. In all these systems, the lack of fluorescent 1:1 complex is related to steric hindrance brought by a methyl group pointing to the naphthalene ring.

A similar addition structure has been calculated for the complex of (1*S*,2*S*)-*N*-methylpseudoephedrine with methyl-2-chloropropionate.[144] The $S_0$–$S_1$ transition of the homochiral complex is shifted to the red of the lines for isolated chromophore, while that of the heterochiral complex is shifted to the blue. Again, the marked difference between the two diastereomers is assigned to stereochemical constraints. The geometry of the heterochiral complex is such that there is a CH···π interaction resulting in a decrease of electrostatic interactions upon electronic excitation, hence a blue shift. In contrast, steric hindrance brought by the methyl group prevents such an interaction to take place in the homochiral pair, resulting in a red-shifted transition.

The observed selectivity is reminiscent of the enantioselective hydrogenation of α and β keto esters on modified catalysts. The catalyst surface is grafted with chiral species, such as naphthalene derivatives, whose molecular plane lies flat on the surface. The modifier forms a 1:1 docking complex with the prochiral keto ester reactant, which in turn forces hydrogenation to occur at one of its faces only.[145,146] In our case, chirality also differentiates the two sides of the ester molecular plane, and only the sterically less-demanding one can approach the naphthalene ring.

No insertion complex is observed in the complexes between α or β-hydroxyacid esters and NapOH, despite insertion being theoretically predicted to be the most stable. The most stable calculated geometry of the (1*S*,2*S*)-*N*-methylpseudoephedrine:(±)-MeLac complexes[144] also corresponds to an insertion complex, in which the internal structure of the chromophore is not strongly affected by complexation: its hydroxy group, still involved in the internal hydrogen bond to the amino group, also interacts with the lactate C=O group, which leads to a bifurcated hydrogen bond. However, the structure of the (1*S*,2*S*)-*N*-methylpseudoephedrine:(±)-MeLac complex has not been determined experimentally and the only experimental evidence of insertion complexes involving *syn* lactates is provided by the methanol:MeLac dimer studied in a slit jet experiment by direct FTIR absorption.[147] Their IR spectrum is characterized by two features which are shifted to the red of both the lactate and methanol absorption. This spectrum indicates formation of an OH···OH bond and its reinforcement through cooperative effects. Comparison with simulated spectra, as well as $^{18}O$ isotope labeling of methanol leads to these bands being attributed to the methanol and MeLac $\nu$(OH) stretch modes of an insertion complex. The hydroxy group of methanol inserts into the internal hydrogen bond of MeLac.

### 3.5. Comparison between Different Systems

The set of experimental results concerning lactic acid and ethanolamine derivatives raises several questions: What is the effect of an aromatic ring on the structure of the complexes, on the size of the formed adduct, and on the chirality discrimination extent? Which parameter dictates formation of addition or insertion complexes? Are there systematic preferences in symmetry or homochiral/heterochiral cluster abundance? To answer these questions both thermodynamic and kinetic aspects of complex formation need to be considered.

#### 3.5.1. Size of the Formed Adducts

As described above, there is a strong enantioselectivity in the size of the adducts formed between NapOH and lactate derivatives. It has been explained in terms of steric hindrance resulting from a methyl group pointing to the naphthalene

  

ring, which hampers formation of a fluorescent 1:1 complex. This system contrasts with its analogue constructed from a benzene chromophore.[64] The homo- and heterochiral adducts with (±)-1-phenyl-1-propanol are both detected in the excitation spectrum, with similar spectroscopic characteristics. However, their excitation spectra do not display the long vibrational progression as observed for the NapOH **IA** complexes. This behavior is probably related to the large polarizability of the naphthalene aromatic ring, which makes it very sensitive to subtle changes in dispersion energy and to the increase in dispersion energy upon electronic excitation.

#### 3.5.2. Insertion or Addition

We have observed different behavior in MeLac dimers and MeMan:MeLac complexes, despite the similarity between the two sets of systems: $C_8$ isomers are dominant in the case of the MeLac or MeGly dimers, while only the less stable $C_5$ form is observed when MeLac or MeGly is associated to MeMan. Similarly, insertion complexes are observed in methanol:MeLac dimers whereas only O-addition complexes are observed with NapOH. Lastly, only addition (on O) or activated addition (on N) complexes are observed in ethanolamine complexes with NapOH, despite insertion being calculated to be energetically more favorable.

From the thermodynamic point of view, insertion complexes generally involve stronger hydrogen-bond interactions than addition complexes, because the two newly formed intermolecular bonds are, taken together, stronger than the two inter- and intramolecular bonds formed in the addition complexes. On the other hand, insertion of a large molecule results in steric hindrance. We expect insertion complexes in small systems (small repulsion, binding energy dominated by electrostatics) and addition in larger systems (strong repulsion, dispersion not negligible). Moreover, the formation of complexes cannot be described by statistical growth; the open form of ethanolamine is not the most stable one but shows a greater affinity to NapOH than the more stable closed form, which makes complexes of the open form more likely.

From a kinetic point of view, the competition between addition and insertion also depends on the reaction barrier for insertion. This barrier correlates with the strength of the intramolecular hydrogen bond. It is easier to open the weak intramolecular hydrogen bond of the *skew* form ($\nu(\mathrm{OH}) = 3641\ \mathrm{cm}^{-1}$) of MeLac than that of its *syn* form, which is stronger ($\nu(\mathrm{OH}) = 3608\ \mathrm{cm}^{-1}$), or that of ethanol amine ($\nu(\mathrm{OH}) = 3569\ \mathrm{cm}^{-1}$). However, there may be concerted reaction paths with a lower activation barrier, if the intermolecular hydrogen bond forms while the intramolecular one is broken.

#### 3.5.3. Cooperative Effects

All the systems involving hydrogen-bonded networks exhibit cooperative effects, which manifest themselves by a frequency lowering of modes involved in both intra- and intermolecular hydrogen bonds or in several intermolecular hydrogen bonds. When forming a complex involving a lactate or an ethanolamine derivative, there is competition between an intramolecular hydrogen bond which is intrinsically strong but isolated and OH···OH or OH···NH intermolecular bonds, which become strong upon cooperative enhancement by forming a homodromic (unidirectional) pattern. Usually, cooperativity wins for larger clusters, but there are stereoselective exceptions which offer stabilizing secondary interactions.[139]

#### 3.5.4. Symmetry Issues

Most dimers of chiral compounds have $C_1$-symmetric structures. If the building blocks are constitutionally identical and larger in number, higher symmetry may arise. Homochiral dimers may assume $C_2$-symmetry and heterochiral dimers can be inversion-symmetric ($C_i$). Pure rotational symmetry ($C_n$) has been found for higher oligomers, if they are homochiral.[93,136] In the case of racemic tetramers, the $S_4$ point group is regularly observed.[139,148] Although these structures do not have a plane of symmetry ($S_1$) or inversion center ($S_2$), they have an improper rotation $S_4$ axis which makes the corresponding cluster assembly achiral. In principle, other point groups are possible, but rarely found. Even such surprising things as achiral dimers from homochiral monomers are conceivable[140] and over the next years we are likely to see attempts to find small model clusters for many of the exotic symmetry cases.

#### 3.5.5. Homochiral and Heterochiral Preferences

In the few characterized clusters built from constitutionally identical monomers, no clear preference for homochiral or heterochiral pairings is evident. This situation is in part due to the fact that relative binding energies are less straightforward to measure than spectral discrimination effects. Macroscopic crystallization experiments are more straightforward and show that enantiophobic molecules,[149] that is, those leading to spontaneous resolution, form a minority. It remains to be seen whether this racemic crystal preference already emerges at the microscopic level.

The formation of neutral homochiral clusters in sublimation enrichment experiments starting from nonracemic mixtures has been postulated.[150] However, classical explanations based on monomer evaporation are also conceivable.[151]

## 4. Chirality Induction

Molecules composed of more than three atoms can always assume chiral geometries. The more atoms, the more likely it is that there are chiral structures in the form of enantiomeric pairs of local minima. Molecules in such configurations are not permanently chiral, unless the racemization barrier between the enantiomers is sufficiently high. By lowering the barrier, parity becomes well defined at some stage and the energy levels split into symmetric and antisymmetric components with respect to inversion. In a time-dependent two-level representation, this corresponds to a periodic tunneling oscillation between the two enantiomers.[11] Thus, the molecule is only transiently chiral. If the barrier vanishes

  

completely, the splitting transforms into a regular vibrational excitation and the molecule only keeps enantiotopic faces, atoms, or lone pairs, it is on average prochiral. In these low-barrier or vanishing-barrier cases, a neighboring permanently chiral object can break the symmetry between the transient enantiomers or enantiotopic faces of the molecule.[152] This phenomenon is called chirality induction, because the permanently chiral object induces chirality in the transiently chiral or prochiral molecule, thus leading to an energy difference between the two directions of approach. Figure 12 also illustrates the third case of a fully achiral

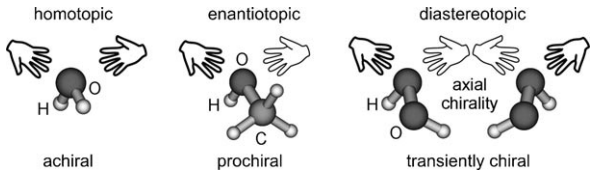


***Figure 12.*** Illustration of the homotopic, enantiotopic, and diastereotopic faces of achiral, prochiral, and transiently chiral molecules, using an example of axial chirality for the transiently chiral molecules. Note that the two faces or lone electron pairs at an HOOH oxygen atom are diastereotopic, while the hydrogen atoms are enantiotopic.

molecule ($H_2O$), which does not lead to an energy difference. In all three cases, chirality information is transferred from the chiral object to the molecule and may be detected at the molecule itself for example, by electronic[153] or vibrational circular dichroism techniques.[154,155] Vibrational circular dichroism is difficult to study for clusters in the gas phase,[156] but it may be applied to matrix-isolated systems,[157] where complexes can be investigated.

Chirality induction is at the heart of modern asymmetric organic synthesis.[145] Permanently chiral reactants or catalysts induce chirality in prochiral or transiently chiral molecules by forming a pre-reaction complex. In the subsequent reaction, which usually involves a sequence of bond breaking or forming steps, a new permanent stereocenter is created in a more or less stereoselective way. Chirality induction is also important in polymer design, where suitable catalysts ensure that the monomers are incorporated into the polymer in a regular way.

### 4.1. The Role of Time Scales and Temperature in Chirality Induction

The distinction between chirality discrimination and chirality induction can be a matter of time scale, in relation to the stereomutation process. On a time scale where the labile unit inverts easily, its complex with a permanently chiral partner may still be configurationally stable. This situation corresponds to a quenching of the tunneling process by the binding partner. On a much shorter time scale, where the labile unit momentarily has a defined chirality sense, the interaction may be classified as being of the chirality discrimination type. In the gas phase, a natural time scale border to decide between the two limiting cases is the upper-ns to lower-μs range. It is the time scale on which cold collisions happen. Molecules which are configurationally labile on this time scale may be better viewed as transiently chiral. They exhibit stereomutation tunneling splittings around 1 MHz or larger, which are also easily measurable by microwave spectroscopy.

Despite the importance of chirality induction in biomolecular and macromolecular synthesis, there are surprisingly few model complexes which have been studied in the gas phase with this aspect in mind. They usually involve axial chirality in alcohols as the labile component and a range of permanently chiral molecules as chirality inducers. The reason is that proton delocalization in these axially chiral molecules can be quenched by complexation, preferentially localizing the molecule in one of the (originally equivalent) minima, whenever this minimum falls significantly below the other one, relative to the size of the tunneling splitting. This effect has structural implications which are easily detected by microwave spectroscopy. Diastereofacial preferences between enantiotopic lone pairs in a prochiral molecule, such as methanol, acting as a hydrogen-bond acceptor towards a chiral hydrogen-bond donor are more difficult to detect even at the low temperatures of a supersonic jet expansion. In room-temperature condensed phases, chirality induction phenomena can only survive if the interactions are strong enough, for example, involving metal coordination or reactive processes after the initial complexation.[158]

### 4.2. Chirality Induction in Axially Chiral Molecules

A detailed theoretical analysis of a clear-cut chirality induction case was carried out by Portmann et al.[89] Chiral *trans*-2,3-dimethyl oxirane was combined with HOOH, forming a single dominant OH···O hydrogen bond along with several secondary interactions. The doubly methylated oxirane unit induces an energy difference (chirodiastaltic energy) of 1.5 kJ mol$^{-1}$ between the two helical HOOH forms. Singly methylated oxirane behaves in a more complex way, as it offers different secondary hydrogen-bond topologies (faces) to HOOH with resulting diastereofacial energy differences.[89] On a very short (picosecond) timescale, the phenomena involved in the recognition between methylated oxirane and HOOH might be classified as chirality discrimination, but we suggest that in such a rapidly interconverting system as HOOH, chirality induction is a better description. Systems such as these may serve as elementary prototypes for chirality amplification by dynamic helices.[159]

Related cases of chirality induction have been studied experimentally with axially chiral ethanol instead of HOOH as a hydrogen-bond donor. The chiral 2,3-dimethyl oxirane example is again straightforward.[160] This molecule favors one of the two helical *gauche* ethanol conformations over the other and also over the achiral *trans* conformation of ethanol (Figure 13). It can be seen how the degeneracy of the tunneling-split *gauche* states of ethanol is lifted by the chiral complexation partner. All three isomers have been detected in the microwave spectrum. The theoretically favored helicity was unambiguously associated with the strongest transitions

  

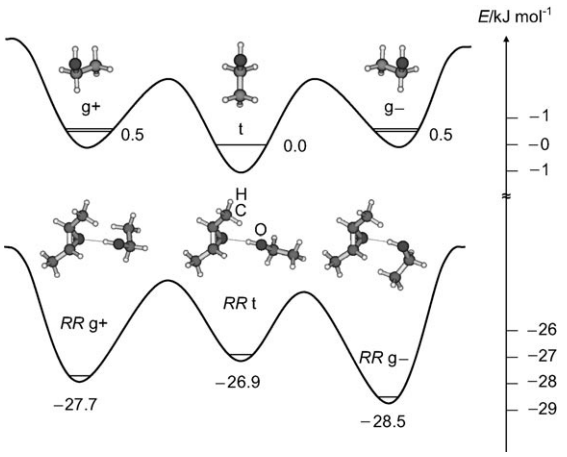


***Figure 13.*** Energy levels of isolated ethanol (and (*R*,*R*)-dimethyl oxirane) and of (*R*,*R*)-dimethyl oxirane/ethanol dimers, as a function of ethanol torsional angle according to MP2/6-311 + G(2d,p) calculations including ZPE.[160] The deficiency in the calculated ethanol t/g energy difference of approximately 0.8 kJ mol$^{-1}$ at this computational level has been corrected. Note that the *gauche* tunneling pair (not to scale) in the unperturbed ethanol molecule changes into two localized states in the g+ and g− wells upon complexation. The connecting 1D adiabatic potentials as a function of ethanol torsional angle are only qualitative.

in the non-equilibrium expansion and confirmed by stagnation pressure and carrier gas variations.[160] The methyl oxirane case is more complex because of the different faces or hydrogen-bond topologies, but the most stable dimer between methyl oxirane and ethanol corresponds to the preferred local environment in the complex of 2,3-dimethyl oxirane with ethanol.[94]

An earlier example involves the complex of 2-naphtyl-1-ethanol with 1-propanol,[66] where a splitting in the fluorescence excitation spectrum has been attributed, on the basis of UV-UV double resonance experiments, to the two enantiomeric gt-1-propanol conformations binding differently to the chiral chromophore. Because monomer racemization involves heavy-atom motion in this case, the conformational lifetime could be in the μs range or longer.[161,162] Therefore, a classification as chirality discrimination would also be justified.

### 4.3. Chirality Induction in Prochiral Molecules

Selection between enantiotopic lone pairs of a prochiral acceptor by a permanently chiral donor has been observed for aromatic chromophores, in which the aromatic OH group is complexed by two methanol molecules.[69,70] The two methanol units form a bridge between the chromophore OH group and the chromophore π-system. Experimental spectra indicate that out of the four possible coordination possibilities at the two methanol units, only a single one is realized at low temperature. Therefore, the chiral chromophore induces a definite chirality in the two complexing prochiral methanol molecules, but the systems are quite flexible.

An even more subtle case of chirality induction and chirality synchronization (see Section 5) can be discussed for isolated methanol clusters. Whereas methanol itself is prochiral, the linear hydrogen-bonded dimer is transiently chiral, depending on which of the enantiotopic electron lone pairs of the acceptor molecule is engaged in the hydrogen bond. Conversion of the enantiomers happens on the ns timescale,[163] as it can be largely accomplished by hydrogen motion. Incorporation of a third methanol molecule can only form a stable cyclic trimer, if at least one of the two newly created stereocenters is of opposite chirality. This phenomenon has recently been shown experimentally.[148] The driving force is the steric repulsion of the methyl groups above and below the hydrogen-bonded ring. In contrast to the dimer, the stereomutation rate of the trimer may already be slow enough to be classified as nontransient, because substantial heavy-atom motion is involved. In the methanol tetramer, an alternating handedness of the four methanol units in the ring is required[148] and it may be assumed that methyl-group tunneling across the ring plane is now even slower. However, another methanol-inverting tunneling process, in which the hydrogen-bonded protons jump concertedly between neighbors should not be dismissed.[148,164] The methanol tetramer has $S_4$ symmetry and is therefore achiral.

### 4.4. Intramolecular Counterparts of Chirality Induction

As there is no strict border between intermolecular and intramolecular bonds, the intramolecular counterpart of chirality induction deserves a brief mention. It involves the transfer of chirality information onto other parts of the molecule, which may be considered prochiral. There is a smooth transition between intramolecular chirality induction and the previously discussed intramolecular chirality discrimination, better known as classical diastereoisomerism.

An intramolecular variant of the methyl oxirane:ethanol or 2-naphtyl-1-ethanol:1-propanol case where a nearby chirality center influences the axial chirality is that of chloropropanol.[113] While the two *gauche* forms are equivalent in 2-chloroethanol or 2-fluoroethanol,[165] replacement of one $C_\alpha$-H atom by a methyl group breaks this symmetry and favors one *gauche* form over the other. In methyl amino ethanol,[125] the three different N-substituents form a transient stereocenter, which is stabilized by an internal OH···N hydrogen bond. In combination with the axial chirality of the backbone, two diastereoisomers are observed in the supersonic jet spectra.

The secondary structure of helical peptides and other foldamers are examples of intramolecular chirality effects. Homoconfigurational peptides are known to form α-helices with a preferred helicity. A small variant is the γ-turn, which can even be established in a capped dipeptide in the gas phase.[166] If only one of the amino acids is chiral, the γ-turn exists in two helicities which are simultaneously observed. However, a specific helicity of the γ-turn is preferred. This phenomenon is a clean case of intramolecular chirality induction by the amino acid stereocenter. If both amino acids are chiral, the γ-turns differ more strongly in energy and only one of them is observed. It is mainly a case of intramolecular chirality discrimination, where helicity induc-

  

tion or folding properties[167] are just secondary effects. These effects have been demonstrated in some recent spectroscopic peptide studies[166,167] but many other examples could be mentioned in this context.[129,168]

A detailed discussion of the formation of stereotactic polymers through chirality induction is beyond the scope of this Review.[158] Aided by a (in most cases, achiral) catalyst, growing polymer chains incorporate further prochiral monomers in a highly stereospecific way. Isotactic and syndiotactic poly(methylmethacrylate)s (PMMAs) may serve as a typical example.[169] Such isotactic and syndiotactic polymers often develop a specific helicity as a secondary consequence of their tacticity. The resulting helical structures can even interact specifically with each other, although the detailed structure of the supramolecular complexes is still under debate.[170]

## 5. Chirality Synchronization

Quartz crystals occur in two enantiomorphic varieties, corresponding to left-handed and right-handed chiral crystal structures which belong to the Sohncke space groups.[171] Although local accumulation effects are known, any global natural difference in abundance between the two crystal forms is at best marginal[172] and could have a number of origins.[11,173] Herein, we address a far simpler issue—that of the existence of both chiral crystal forms despite the achiral nature of its building blocks, namely symmetric $SiO_4$ tetrahedra. Although the formation process of quartz crystals is certainly complex, there must be key steps involved, in which neighboring tetrahedra synchronize their subtle distortions in such a way that a definite chirality of their assembly emerges. This phenomenon may be called chirality synchronization. Other achiral molecules, such as glycine, can crystallize in a centrosymmetric arrangement ($\alpha$-glycine) such that layers of molecules with a left-handed and a right-handed environment alternate.[174] Again, there is some synchronization of the transient (supra)molecular chirality involved, although in the case of glycine the net-effect is an achiral assembly, because constructive chirality synchronization is restricted to two dimensions. Spontaneous resolution[149] is indeed more frequent in two dimensions[175,176] than it is in three-dimensional space.[174] Chirality synchronization phenomena are of practical importance, because the emerging macroscopic assemblies can later be used for enantioselective processes,[174] that is, for chirality induction.[177,178] A particularly extreme case of chirality synchronization is that of sodium chlorate,[179] an achiral compound which crystallizes in enantiomeric crystals. Starting from a racemic suspension of such crystals, continuous grinding and stirring ultimately leads to total 'de facto' symmetry breaking,[173] that is, to enantiopure crystals.

Unfortunately, crystal structures and crystallization behavior are notoriously difficult to predict. The roots of chirality synchronization are therefore more easily studied in the gas phase, where related phenomena may also be found. Instead of covalent bonds as in quartz, hydrogen bonds are used to make the connections. Helical building blocks require a minimum of four atoms. Therefore, HOOH, $H_2N{-}NH_2$ and its homologues are among the simplest representatives.[180,181]

In the vibrational ground state, HOOH converts between left- and right-handed helices on a timescale of 3 ps (full oscillation period)[182] after being localized in one of the helicities. Its dimer features two equivalent hydrogen bonds and is presumably centrosymmetric, that is, it involves monomers of opposite helicity.[183] However, the dimer built from monomers with the same helicity is predicted to be close in energy.[184,185] No spectroscopic data for the vacuum isolated dimer are known and it is unclear to which degree the stereomutation process is quenched by the symmetric hydrogen bonds. Larger clusters of HOOH (starting at four monomers) are predicted to synchronize their helicity in beautiful supramolecular structures.[184,185]

In ethanol, the two enantiomeric *gauche* forms are approximately 0.5 kJ mol$^{-1}$ less stable than the *trans* form and interconvert rapidly, on a 10 ps time scale.[186] When two ethanol molecules form a hydrogen-bonded complex with well-defined acceptor and donor roles, the stereomutation is largely quenched[187] and a rich conformational diversity arises. Up to six enantiomeric pairs of dimer conformations might be observable in a supersonic jet expansion.[188] Their energy sequence is found to be very subtle, the global minimum being predicted to be tg,[189,190] tt,[191] gt[187,192] or gg[188] in turn. The pairing preferences in condensed phases also differ. Solid ethanol is known to consist of hydrogen-bonded chains involving alternating g and t conformations.[193] In a cryogenic Ar matrix ethanol dimers prefer a tt conformation,[190] but other conformations are also found.

Two groups have independently investigated the conformational diversity of ethanol dimers by recording their IR absorption spectrum using different jet expansion techniques.[72,192] The dimer O–H stretching spectra obtained by the two techniques consist of a triplet of equally spaced absorption peaks, the central one possibly representing a closely spaced doublet. Thus, experiment suggests a minimum of three to four conformations present in the low-temperature expansion, either corresponding to a thermal Boltzmann population or being trapped behind sufficiently high barriers. Complementary experiments suggest that the height of such trapping barriers must be $\geq 3$ kJ mol$^{-1}$. The multiplicity of dimer conformations in supersonic jet expansions was recently confirmed by Raman spectroscopy[138] and three dimer structures could be structurally elucidated by microwave spectroscopy.[187]

Conformational relaxation can be promoted by the addition of argon traces to the carrier gas.[52] Only a single spectral peak survives in the IR spectrum and must therefore correspond to the most stable conformation, including zero-point-energy effects. Elaborate calculations[52,187] suggest that it is indeed a dimer in which both ethanol units adopt a *gauche* conformation with the same helicity or chirality sense. Thus, two achiral monomers preferentially form a homoconformational chiral dimer in a most elementary model of the formation of helicity in quartz. However, the energetic difference to nonsynchronized conformations is very small, as intermolecular recognition in ethanol dimers only involves a single strong contact.

Replacement of one methyl hydrogen atom by fluorine in 2-monofluoroethanol (MFE) has two major effects. It stabil-

izes the OH group of the monomer in two transiently chiral *gauche* conformations through a weak intramolecular O–H···F contact and it provides a second intermolecular binding site. Being sterically similar to, but electrostatically very different from hydrogen, fluorine is often used to modify intermolecular recognition. MFE dimers occur in two hydrogen-bond topologies, with the more stable one being of the inserted type.[165] In this system, there appears to be a slight preference for opposite helicity in the two building blocks. Owing to the μs or longer timescale of the stereomutation process in MFE monomers,[194] MFE dimers may be considered as a case of chirality discrimination.

A more interesting behavior is observed for 2,2,2-trifluoroethanol (TFE, Figure 14). The monomer oscillates between the two enantiomeric *gauche* forms with a 170 ps period, which is much slower than for ethanol[195] but orders of magnitude faster than MFE because the process is largely limited to hydrogen atom motion. Two different hydrogen-bond topologies can be realized in the dimer.[196,197] The calculations predict an almost perfect energetic balance between an inserted structure with synchronized helicity and an addition structure with opposite helicity, separated by relatively high ($\geq 5\,\mathrm{kJ\,mol^{-1}}$) barriers. Nevertheless, even under the mildest jet relaxation conditions, only the inserted structure with constructive chirality synchronization could be detected (see Figure 14). Larger clusters show a tendency to stabilize *trans* conformations,[196] which are also quite abundant in the liquid.[198] Interestingly, such clusters of fluoroalcohols play an important role in accelerating stereospecific reactions of another helical molecule, HOOH, with olefins.[199] Furthermore, there is a pronounced promotion of helicity in peptides when trifluoroethanol is added as a cosolvent.[200] Quite generally, trifluoromethyl groups can have major implications on intermolecular recognition phenomena[201] presumably because of their electrostatic tendency to repel each other.

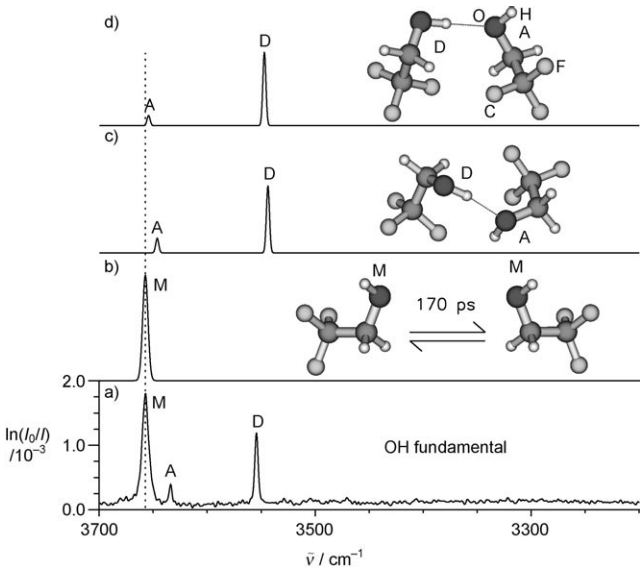


***Figure 14.*** Experimental OH stretching-frequency jet FTIR spectrum of the TFE monomer (M) and the hydrogen-bond donor (D)/acceptor (A) modes of a single-dimer conformation (bottom trace). Spectral simulations based on harmonic MP2/6-311 + G* calculations are shown for the racemizing monomer and for two energetically favorable dimers (insertion structure shown in (c) addition structure shown in (d)). Only the homochiral insertion dimer with an OH···F hydrogen bond is detected in a case of chirality synchronization.[197]

We close this Section with an interesting intramolecular counterpart of chirality synchronization. Isolated linear *n*-alkanes have an energetic preference for the stretched, achiral, all-*trans* conformation. With increasing *n* value, there will be a growing number of low-lying torsional states which involve some *gauche* angles. Ultimately, some of these bent conformations will become more stable than the all-*trans* conformation, because they profit from intrachain dispersion interactions. The critical *n* value at which this happens is currently under debate.[141,202] A favorable torsional subsequence which allows for attractive intrachain interactions is …tggtggt…, halfway along the chain. To align the two chain segments, all four *gauche* torsions need to have the same helicity. Hence, dispersion-driven alkane chain folding is an intrachain chirality synchronization process. It would be of interest to know at which chain length *n* the folded structure becomes more stable than the stretched one. The transition from stretched to folded may happen as early as $C_{14}H_{30}$, according to preliminary MP2 calculations (see Figure 15).[203]

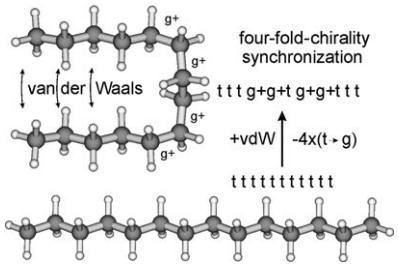


***Figure 15.*** Dispersion interactions drive the folding of all-*trans* *n*-alkanes starting at a critical chain length approximately 14 through a four-fold *trans–gauche* isomerization of the central torsion angles. For an energetically favorable chain conformation, it is essential that all four twisting angles have the same sign.

Any experimental data on this number could provide important benchmarks for accurate ab initio calculations. Such experiments are not simple but rather correspond to finding a needle (the all-*trans* conformation) in a haystack of all the other thermally populated conformations and then studying its temperature dependence. Supersonic jet Raman spectroscopy[162] monitoring the characteristic accordion vibration of the all-*trans* structure[204] holds some promise in this field.

## 6. Conclusions

In this Review chirality recognition phenomena between neutral molecules have been classified into three categories,

  

depending on whether both, one, or none of the molecular components may be considered to be permanently chiral.

The exchange of the term "chirality" by "polarity" may help to unravel certain parallels to the fundamental long-range mechanisms of intermolecular interaction. Chirality discrimination is based on permanently chiral molecules, in analogy to classical electrostatic interactions, which are built on permanent dipole and higher multipole moments. Chirality-induction phenomena parallel dipole induction by inducing a new property (chirality/polarity) in a molecule through its interaction with another molecule which already possesses this property. Chirality synchronization is a more subtle phenomenon in which transient chiral conformations are synchronized among neighboring molecules, much like fluctuating dipoles cause dispersion interactions between nonpolar moieties. The role of electronic polarizability is now taken by molecular fluxionality. Even the quantum character of dispersion interactions finds an occasional parallel in tunneling processes which connect helical conformations in systems, such as hydrogen peroxide or alcohols. Like intermolecular interactions in general, these chirality recognition effects may superimpose each other. Chirality discrimination between permanently chiral molecular objects is often linked to induced phenomena, such as conformational changes, which are able to enhance the rigid molecule effects (induced fit). The ability of a molecule to engage in chirality synchronization is favorable for its susceptibility to chirality-induction phenomena and also allows for a transmission of chirality information over larger distances.

The elementary chirality-recognition processes which we have discussed in the low-temperature gas phase may be amplified to multicontact supramolecular phenomena in the condensed phase. They are then able to persist at temperatures relevant in the life sciences and in polymer materials. A reductionist approach to the complex phenomenology of soft matter can always profit from spectroscopic insights into the behavior of primary building blocks.

Undoubtedly, chirality recognition is one of the most appealing aspects of intermolecular interactions. The latter have been characterized in enormous depth and detail by supersonic jet spectroscopy ever since the early 1970s. Chiral species have entered this scene in the mid 1990s. More than ten years later, there are still many new phenomena to be discovered and analyzed, but several systematic trends start to emerge. This Review has tried to identify and summarize some of them, and to draw parallels to solution or solid-state chemistry.

Chiral-phase chromatography experiments show that enantiomer separation can be achieved provided that the molecule to separate occurs in at least one conformer showing enantioselective interactions with the stationary phase.[26] Similarly in the gas phase, chirality-discrimination efficiency depends on the conformation of the species at play. Moreover, the observed gas phase complexes are not always made from the most stable conformer of the subunits. The structures of the subunits adapt to each other in a concerted way, to optimize the interaction energy, in particular non-additive interactions (cooperative effects). This situation is reminiscent of the induced-fit phenomenon observed in biological macromolecules.

The microscopic recognition phenomena which we have discussed also have their parallels in the macroscopic world of solids. Chirality discrimination is what Pasteur ultimately did when he picked out the "right" crystals from the conglomerate of tartrate crystals using his tweezers, eyes, and brain. Chirality induction happens when we seed a silica melt with a chiral quartz crystal, to obtain a collection of enantiopure crystals. Chirality induction also manifests itself in supramolecular chemistry: doping an achiral nematic phase with an enantiopure solute induces formation of a chiral cholesteric phase, the pitch of which depends on the solute–solvent couple.[205] Chirality synchronization occurs when a suspension of right- and left-handed sodium chlorate crystals is converted into right- or left-handed crystals only, upon mechanical milling and stirring.[179] In all these cases, the phenomena may change qualitatively as a function of length scale,[206] making cluster approaches particularly important for their detailed characterization.

Theoretical modeling of the simplest experimental model systems is possible, but difficult in the field of chirality recognition. Being a subtle difference between relatively large interaction energies, even the correct sign of the chirodiastaltic energy may be hard to predict in some instances. Therefore, the experimental work presented herein offers some of the most interesting challenges to quantum chemistry.

There is growing interest in the study of biologically relevant molecules in the gas phase. Methods such as expansion from supercritical solutions,[207] laser evaporation from a solid or a frozen solution help to study molecules of increasing complexity.[46,208–211] Aggregates of oligofunctional chiral molecules involving hydrogen-bonded networks, up to and including peptide model dimers[212] are of special interest. The next decade is therefore expected to witness an increase in complexity and diversity of the neutral gas-phase systems investigated, bringing the field even closer to the condensed-phase phenomena which it tries to model. This next decade may also witness the first spectroscopic evidence for parity violation in chiral molecules. In contrast to chirality recognition, where vacuum isolation offers fundamental insights into a phenomenon which has been exploited in the condensed phase for many decades, vacuum isolation appears absolutely essential to detect this extremely subtle effect and technological advances are vital, now that the concepts for such experiments have been put forward.[213]

*We thank our co-workers and colleagues for their contributions, which are reflected in the list of references. In particular, warm thanks are due to Dr. K. Le Barbu-Debus for her decisive contribution to part of the work presented. Similarly, Dr. N. Borho deserves particular credit for having started and sustained the later chirality recognition studies in Göttingen and for assistance with some of the Figures. Financial support over many years from CNRS and the DFG (SFB 357, Su 121/2) and the FCI is gratefully acknowledged. This review is justly dedicated to M. Quack, the academic teacher of one of us, on the occasion of his 60th birthday. Born 100 years after the*

  

*"annus mirabilis" for stereochemistry,[116] his research focus is on the subtle role of parity violating forces in molecular chirality.*

Received: February 27, 2008
Published online: August 11, 2008

[1] J. Podlech, *Cell. Mol. Life Sci.* **2001**, *58*, 44.
[2] L. Pasteur, *Leçons de chimie professées en 1860 par MM. Pasteur, Cahours, Wurtz, Berthelot, Sainte-Claire Devile, Barral et Dumas*, Hachette, Paris, **1861**.
[3] T. D. Lee, C. N. Yang, *Phys. Rev.* **1956**, *104*, 254.
[4] C. S. Wu, E. Ambler, R. W. Hayward, D. D. Hoppes, R. P. Hudson, *Phys. Rev.* **1957**, *105*, 1413.
[5] Y. Yamagata, *J. Theor. Biol.* **1966**, *11*, 495.
[6] R. Bast, P. Schwerdtfeger, T. Saue, *J. Chem. Phys.* **2006**, *125*, 064504.
[7] A. Bakasov, T. K. Ha, M. Quack, *J. Chem. Phys.* **1998**, *109*, 7263; A. Bakasov, T. K. Ha, M. Quack, *J. Chem. Phys.* **1999**, *110*, 6081.
[8] M. Quack, J. Stohner, M. Willeke, *Annu. Rev. Phys. Chem.* **2008**, *59*, 741.
[9] M. Quack, *Chem. Phys. Lett.* **1986**, *132*, 147; M. Quack, M. Willeke, *J. Phys. Chem. A* **2006**, *110*, 3338.
[10] J. Crassous, C. Chardonnet, T. Saue, P. Schwerdtfeger, *Org. Biomol. Chem.* **2005**, *3*, 2218.
[11] M. Quack, *Angew. Chem.* **2002**, *114*, 4812; *Angew. Chem. Int. Ed.* **2002**, *41*, 4618.
[12] S. C. Stinson, *Chem. Eng. News* **2001**, *79*, 79.
[13] T. H. Webb, C. S. Wilcox, *Chem. Soc. Rev.* **1993**, *22*, 383.
[14] M. Tsukamoto, H. B. Kagan, *Adv. Synth. Catal.* **2002**, *344*, 453.
[15] R. Mehvar, D. R. Brocks, *J. Pharm. Pharm. Sci.* **2001**, *4*, 185.
[16] R. Bentley, *Chem. Rev.* **2006**, *106*, 4099.
[17] IUPAC Compendium of Chemical Terminology Electronic Version, http://goldbook.iupac.org/C01058.html.
[18] L. J. Prins, J. Huskens, F. de Jong, P. Timmerman, D. N. Reinhoudt, *Nature* **1999**, *398*, 498.
[19] M. Kempe, K. Mosbach, *J. Chromatogr. A* **1995**, *694*, 3.
[20] N. Berova, K. Nakanishi, R. W. Woody, *Circular Dichroism. Principle and Applications*, Wiley, New York, **2000**.
[21] M. Rekharsky, Y. Inoue, *J. Am. Chem. Soc.* **2000**, *122*, 4418.
[22] K. B. Lipkowitz, S. Raghothama, J. Yang, *J. Am. Chem. Soc.* **1992**, *114*, 1554.
[23] L. Pu, *Chem. Rev.* **2004**, *104*, 1687.
[24] E. Fischer, *Ber. Dtsch. Chem. Ges.* **1894**, *27*, 2985.
[25] A. G. Ogstron, *Nature* **1948**, *162*, 963.
[26] W. H. Pirkle, T. C. Pochapsky, *Chem. Rev.* **1989**, *89*, 347.
[27] S. Garten, P. U. Biedermann, I. Agranat, S. Topiol, *Chirality* **2005**, *17*, S159.
[28] T. P. Radhakrishnan, S. Topiol, P. U. Biedermann, S. Garten, I. Agranat, *Chem. Commun.* **2002**, 2664.
[29] S. Topiol, *Chirality* **1989**, *1*, 69.
[30] S. Topiol, M. Sabio, *J. Am. Chem. Soc.* **1989**, *111*, 4109.
[31] G. Subramanian, *Chiral separation techniques*, 3rd ed., Wiley-VCH, Weinheim, **2001**.
[32] R. G. Cooks, T. L. Kruger, *J. Am. Chem. Soc.* **1977**, *99*, 1279.
[33] W. A. Tao, R. G. Cooks, *Anal. Chem.* **2003**, *75*, 25A.
[34] J. Ramirez, F. He, C. B. Lebrilla, *J. Am. Chem. Soc.* **1998**, *120*, 7387.
[35] Y. J. Liang, J. S. Bradshaw, D. V. Dearden, *J. Phys. Chem. A* **2002**, *106*, 9665.
[36] C. A. Schalley, *Mass Spectrom. Rev.* **2001**, *20*, 253.
[37] M. Sawada, *Mass Spectrom. Rev.* **1997**, *16*, 73.
[38] M. Speranza, *Int. J. Mass Spectrom.* **2004**, *232*, 277.
[39] H. A. Cox, R. Hodyss, J. L. Beauchamp, *J. Am. Chem. Soc.* **2005**, *127*, 4078.
[40] X. L. Kong, I. A. Tsai, S. Sabu, C. C. Han, Y. T. Lee, H. C. Chang, S. Y. Tu, A. H. Kung, C. C. Wu, *Angew. Chem.* **2006**, *118*, 4236; *Angew. Chem. Int. Ed.* **2006**, *45*, 4130.
[41] P. Yang, R. Xu, S. C. Nanita, R. G. Cooks, *J. Am. Chem. Soc.* **2006**, *128*, 17074.
[42] M. Speranza, M. Satta, S. Piccirillo, F. Rondino, A. Paladini, A. Giardini, A. Filippi, D. Catone, *Mass Spectrom. Rev.* **2005**, *24*, 588.
[43] G. A. Hembury, V. V. Borovkov, Y. Inoue, *Chem. Rev.* **2008**, *108*, 1.
[44] R. E. Smalley, D. H. Levy, L. Wharton, *J. Chem. Phys.* **1976**, *64*, 3266.
[45] P. D. Godfrey, R. D. Brown, F. M. Rodgers, *J. Mol. Struct.* **1996**, *376*, 65.
[46] B. C. Dian, G. M. Florio, J. R. Clarkson, A. Longarte, T. S. Zwier, *J. Chem. Phys.* **2004**, *120*, 9033.
[47] B. C. Dian, A. Longarte, P. Winter, T. S. Zwier, *J. Chem. Phys.* **2004**, *120*, 133.
[48] J. Clarkson, B. C. Dian, L. Moriggi, A. DeFusco, V. McCarthy, K. Jordan, T. S. Zwier, *J. Chem. Phys.* **2005**, *122*, 214311.
[49] D. J. Wales, J. P. K. Doye, M. A. Miller, P. N. Mortenson, T. R. Walsh, *Adv. Chem. Phys.* **2000**, *115*, 1.
[50] P. Felder, H. H. Günthard, *Chem. Phys.* **1982**, *71*, 9.
[51] R. S. Ruoff, T. D. Klots, T. Emilsson, H. S. Gutowsky, *J. Chem. Phys.* **1990**, *93*, 3142.
[52] C. Emmeluth, V. Dyczmons, T. Kinzel, P. Botschwina, M. A. Suhm, M. Yanez, *Phys. Chem. Chem. Phys.* **2005**, *7*, 991.
[53] D. L. Osborn, J. C. Alfano, N. Vandantzig, D. H. Levy, *J. Chem. Phys.* **1992**, *97*, 2276.
[54] J. C. Alfano, S. J. Martinez, D. H. Levy, *J. Chem. Phys.* **1992**, *96*, 2522.
[55] C. L. Morter, Y. R. Wu, D. H. Levy, *J. Chem. Phys.* **1991**, *95*, 1518.
[56] H. T. Jonkman, U. Even, J. Kommandeur, *J. Phys. Chem.* **1985**, *89*, 4240.
[57] M. D. Brookes, D. J. Hughes, B. J. Howard, *J. Chem. Phys.* **1996**, *104*, 5391.
[58] A. Bastida, J. Zuniga, A. Requena, B. Miguel, J. A. Beswick, J. Vigue, N. Halberstadt, *J. Chem. Phys.* **2002**, *116*, 1944.
[59] U. Erlekam, M. Frankowski, G. von Helden, G. Meijer, *Phys. Chem. Chem. Phys.* **2007**, *9*, 3786.
[60] A. R. Al Rabaa, E. Bréhéret, F. Lahmani, A. Zehnacker, *Chem. Phys. Lett.* **1995**, *237*, 480.
[61] A. Giardini-Guidoni, S. Piccirillo, *Isr. J. Chem.* **1997**, *37*, 439.
[62] A. Al Rabaa, K. Le Barbu, F. Lahmani, A. Zehnacker-Rentien, *J. Phys. Chem. A* **1997**, *101*, 3273.
[63] A. Giardini-Guidoni, S. Piccirillo, D. Scuderi, M. Satta, T. M. D. Palma, M. Speranza, *Phys. Chem. Chem. Phys.* **2000**, *2*, 4139.
[64] A. Giardini-Guidoni, A. Paladini, F. Rondino, S. Piccirillo, M. Satta, M. Speranza, *Org. Biomol. Chem.* **2005**, *3*, 3984.
[65] S. Piccirillo, F. Rondino, D. Catone, A. G. Guidoni, A. Paladini, M. Tacconi, M. Satta, M. Speranza, *J. Phys. Chem. A* **2005**, *109*, 1828.
[66] K. Le Barbu, V. Brenner, P. Millié, F. Lahmani, A. Zehnacker-Rentien, *J. Phys. Chem. A* **1998**, *102*, 128.
[67] D. Scuderi, A. Paladini, S. Piccirillo, M. Satta, D. Catone, A. Giardini, A. Filippi, M. Speranza, *Chem. Commun.* **2002**, 2438.
[68] K. Le Barbu, F. Lahmani, M. Mons, M. Broquier, A. Zehnacker, *Phys. Chem. Chem. Phys.* **2001**, *3*, 4684.
[69] K. Le Barbu-Debus, N. Seurre, F. Lahmani, A. Zehnacker-Rentien, *Phys. Chem. Chem. Phys.* **2002**, *4*, 4866.
[70] N. Seurre, J. Sepiol, F. Lahmani, A. Zehnacker-Rentien, K. Le Barbu-Debus, *Phys. Chem. Chem. Phys.* **2004**, *6*, 4658.
[71] M. Mons, F. Piuzzi, I. Dimicoli, A. Zehnacker, F. Lahmani, *Phys. Chem. Chem. Phys.* **2000**, *2*, 5065.
[72] T. Häber, U. Schmitt, M. A. Suhm, *Phys. Chem. Chem. Phys.* **1999**, *1*, 5573.

  

[73] D. Zimmermann, T. Häber, H. Schaal, M. A. Suhm, *Mol. Phys.* **2001**, *99*, 413.
[74] A. Beil, D. Luckhaus, M. Quack, *Ber. Bunsen-Ges.* **1996**, *100*, 1853.
[75] H. Schaal, T. Häber, M. A. Suhm, *J. Phys. Chem. A* **2000**, *104*, 265.
[76] M. Farnik, C. Steinbach, M. Weimann, U. Buck, N. Borho, M. A. Suhm, *Phys. Chem. Chem. Phys.* **2004**, *6*, 4614.
[77] S. Tanabe, T. Ebata, M. Fujii, N. Mikami, *Chem. Phys. Lett.* **1993**, *215*, 347.
[78] R. N. Pribble, A. W. Garrett, K. Haber, T. S. Zwier, *J. Chem. Phys.* **1995**, *103*, 531.
[79] C. Riehn, C. Lahmann, B. Wassermann, B. Brutschy, *Chem. Phys. Lett.* **1992**, *197*, 443.
[80] M. Broquier, F. Lahmani, A. Zehnacker-Rentien, V. Brenner, P. Millié, A. Peremans, *J. Phys. Chem. A* **2001**, *105*, 6841.
[81] F. Lahmani, A. Zehnacker-Rentien, M. Broquier, *J. Photochem. Photobiol. A* **2002**, *154*, 41.
[82] F. Lahmani, M. Broquier, A. Zehnacker-Rentien, *Chem. Phys. Lett.* **2002**, *354*, 337.
[83] N. Seurre, K. Le Barbu-Debus, F. Lahmani, A. Zehnacker-Rentien, J. Sepiol, *Chem. Phys.* **2003**, *295*, 21.
[84] K. R. Leopold, G. T. Fraser, S. E. Novick, W. Klemperer, *Chem. Rev.* **1994**, *94*, 1807.
[85] B. Velino, P. Ottaviani, W. Caminati, A. Giardini, A. Paladini, *ChemPhysChem* **2006**, *7*, 565.
[86] D. Scuderi, A. Paladini, M. Satta, D. Catone, S. Piccirillo, M. Speranza, A. G. Guidoni, *Phys. Chem. Chem. Phys.* **2002**, *4*, 4999.
[87] K. Le Barbu-Debus, F. Lahmani, A. Zehnacker-Rentien, N. Guchhait, S. S. Panja, T. Chakraborty, *J. Chem. Phys.* **2006**, *125*, 174305.
[88] D. P. Craig, D. P. Mellor, *Top. Curr. Chem.* **1976**, *63*, 1.
[89] S. Portmann, A. Inauen, H. P. Luthi, S. Leutwyler, *J. Chem. Phys.* **2000**, *113*, 9577.
[90] L. Alkorta, O. Picazo, J. Elguero, *Curr. Org. Chem.* **2006**, *10*, 695.
[91] P. Zielke, M. A. Suhm, *Phys. Chem. Chem. Phys.* **2007**, *9*, 4528.
[92] Z. Su, N. Borho, Y. J. Xu, *J. Am. Chem. Soc.* **2006**, *128*, 17126.
[93] N. Borho, M. A. Suhm, *Phys. Chem. Chem. Phys.* **2004**, *6*, 2885.
[94] N. Borho, Y. J. Xu, *Angew. Chem.* **2007**, *119*, 2326; *Angew. Chem. Int. Ed.* **2007**, *46*, 2276.
[95] A. K. King, B. J. Howard, *Chem. Phys. Lett.* **2001**, *348*, 343.
[96] V. Brenner, A. Zehnacker, F. Lahmani, P. Millié, *J. Phys. Chem.* **1993**, *97*, 10570.
[97] V. Brenner, P. Millié, *Z. Phys. D* **1994**, *30*, 327.
[98] A. Latini, M. Satta, A. Giardini-Guidoni, S. Piccirillo, M. Speranza, *Chem. Eur. J.* **2000**, *6*, 1042.
[99] N. Seurre, J. Sepiol, K. Le Barbu-Debus, F. Lahmani, A. Zehnacker-Rentien, *Phys. Chem. Chem. Phys.* **2004**, *6*, 2867.
[100] K. Le Barbu-Debus, M. Broquier, A. Mahjoub, A. Zehnacker-Rentien, *J. Phys. Chem. A. 2008*, in press.
[101] K. Le Barbu, F. Lahmani, A. Zehnacker-Rentien, *J. Phys. Chem. A* **2002**, *106*, 6271.
[102] N. Seurre, K. Le Barbu-Debus, F. Lahmani, A. Zehnacker-Rentien, J. Sepiol, *J. Mol. Struct.* **2004**, *692*, 127.
[103] K. Le Barbu-Debus, M. Broquier, F. Lahmani, A. Zehnacker-Rentien, *Mol. Phys.* **2005**, *103*, 1655.
[104] W. H. Pirkle, T. C. Pochapsky, *J. Am. Chem. Soc.* **1987**, *109*, 5975.
[105] K. Akasaka, K. Gyimesi-Forras, M. Lammerhofer, T. Fujita, M. Watanabe, N. Harada, W. Lindner, *Chirality* **2005**, *17*, 544.
[106] F. Lahmani, K. Le Barbu-Debus, N. Seurre, A. Zehnacker-Rentien, *Chem. Phys. Lett.* **2003**, *375*, 636.
[107] A. R. AlRabaa, K. Le Barbu, F. Lahmani, A. Zehnacker-Rentien, *J. Photochem. Photobiol. A* **1997**, *105*, 277.
[108] F. Lahmani, K. Le Barbu, A. Zehnacker-Rentien, *J. Phys. Chem. A* **1999**, *103*, 1991.
[109] T. Suzuki, M. Sato, N. Mikami, M. Ito, *Chem. Phys. Lett.* **1986**, *127*, 292.
[110] F. Lahmani, E. Bréhéret, A. Zehnacker-Rentien, T. Ebata, *J. Chem. Soc. Faraday Trans.* **1993**, *89*, 623.
[111] S. Speiser, *Chem. Rev.* **1996**, *96*, 1953.
[112] J. D. Swalen, D. R. Herschbach, *J. Chem. Phys.* **1957**, *27*, 100.
[113] T. Goldstein, M. S. Snow, B. J. Howard, *J. Mol. Spectrosc.* **2006**, *236*, 1.
[114] N. Borho, T. Häber, M. A. Suhm, *Phys. Chem. Chem. Phys.* **2001**, *3*, 1945.
[115] N. Borho, M. A. Suhm, *Phys. Chem. Chem. Phys.* **2002**, *4*, 2721.
[116] K. Mislow, *Top. Stereochem.* **1999**, *22*, 1.
[117] A. K. King, B. J. Howard, *J. Mol. Spectrosc.* **2001**, *205*, 38.
[118] N. Borho, Diploma Thesis, Göttingen, **2001**.
[119] A. Filippi, A. Giardini, A. Latini, S. Piccirillo, D. Scuderi, M. Speranza, *Int. J. Mass Spectrom.* **2001**, *210*, 483.
[120] A. Latini, D. Toja, A. Giardini-Guidoni, S. Piccirillo, M. Speranza, *Angew. Chem.* **1999**, *111*, 838; *Angew. Chem. Int. Ed.* **1999**, *38*, 815.
[121] J. Paul, I. Hearn, B. J. Howard, *Mol. Phys.* **2007**, *105*, 825.
[122] D. Scuderi, A. Paladini, M. Satta, D. Catone, F. Rondino, M. Tacconi, A. Filippi, S. Piccirillo, A. Giardini-Guidoni, M. Speranza, *Phys. Chem. Chem. Phys.* **2003**, *5*, 4570.
[123] C. Cacela, R. Fausto, M. L. Duarte, *Vib. Spectrosc.* **2001**, *26*, 113.
[124] R. Fausto, C. Cacela, M. L. Duarte, *J. Mol. Struct.* **2000**, *550*, 365.
[125] Y. Q. Liu, C. A. Rice, M. A. Suhm, *Can. J. Chem.* **2004**, *82*, 1006.
[126] N. A. Macleod, J. P. Simons, *Phys. Chem. Chem. Phys.* **2003**, *5*, 1123.
[127] N. A. Macleod, E. G. Robertson, J. P. Simons, *Mol. Phys.* **2003**, *101*, 2199.
[128] P. Butz, R. T. Kroemer, N. A. Macleod, E. G. Robertson, J. P. Simons, *J. Phys. Chem. A* **2001**, *105*, 1050.
[129] P. Butz, R. T. Kroemer, N. A. Macleod, J. P. Simons, *Phys. Chem. Chem. Phys.* **2002**, *4*, 3566.
[130] K. Le Barbu-Debus, F. Lahmani, A. Zehnacker-Rentien, N. Guchhait, *Chem. Phys. Lett.* **2006**, *422*, 218.
[131] R. J. Graham, R. T. Kroemer, M. Mons, E. G. Robertson, L. C. Snoek, J. P. Simons, *J. Phys. Chem. A* **1999**, *103*, 9706.
[132] L. Pauling, *Chem. Eng. News* **1946**, *24*, 1375.
[133] M. S. Taylor, E. N. Jacobsen, *Angew. Chem.* **2006**, *118*, 1550; *Angew. Chem. Int. Ed.* **2006**, *45*, 1520.
[134] A. Borba, A. Gomez-Zavaglia, L. Lapinski, R. Fausto, *Vib. Spectrosc.* **2004**, *36*, 79.
[135] P. Ottaviani, B. Velino, W. Caminati, *Chem. Phys. Lett.* **2006**, *428*, 236.
[136] N. Borho, M. A. Suhm, *Org. Biomol. Chem.* **2003**, *1*, 4351.
[137] M. Farnik, M. Weimann, C. Steinbach, U. Buck, N. Borho, T. B. Adler, M. A. Suhm, *Phys. Chem. Chem. Phys.* **2006**, *8*, 1148.
[138] P. Zielke, M. A. Suhm, *Phys. Chem. Chem. Phys.* **2006**, *8*, 2826.
[139] T. B. Adler, N. Borho, M. Reiher, M. A. Suhm, *Angew. Chem.* **2006**, *118*, 3518; *Angew. Chem. Int. Ed.* **2006**, *45*, 3440.
[140] F. A. Anet, S. S. Miura, J. Siegel, K. Mislow, *J. Am. Chem. Soc.* **1983**, *105*, 1419.
[141] T. Schwabe, S. Grimme, *Phys. Chem. Chem. Phys.* **2007**, *9*, 3397.
[142] H. N. Bordallo, B. A. Kolesov, E. V. Boldyreva, F. Juranyi, *J. Am. Chem. Soc.* **2007**, *129*, 10984.
[143] N. Seurre, K. Le Barbu-Debus, F. Lahmani, A. Zehnacker, N. Borho, M. A. Suhm, *Phys. Chem. Chem. Phys.* **2006**, *8*, 1007.
[144] A. Giardini-Guidoni, A. Paladini, S. Piccirillo, F. Rondino, M. Satta, M. Speranza, *Org. Biomol. Chem.* **2006**, *4*, 2012.
[145] A. Vargas, T. Bürgi, A. Baiker, *J. Catal.* **2004**, *226*, 69.
[146] M. Jacoby, *Chem. Eng. News* **2002**, *80*, 43.

  

[147] N. Borho, M. A. Suhm, K. Le Barbu-Debus, A. Zehnacker, *Phys. Chem. Chem. Phys.* **2006**, *8*, 4449.
[148] R. W. Larsen, P. Zielke, M. A. Suhm, *J. Chem. Phys.* **2007**, *126*, 194307.
[149] L. Perez-Garcia, D. B. Amabilino, *Chem. Soc. Rev.* **2007**, *36*, 941.
[150] R. H. Perry, C. P. Wu, M. Nefliu, R. G. Cooks, *Chem. Commun.* **2007**, 1071.
[151] D. L. Garin, G. Cooke, J. Forothy, L. Kelly, *J. Org. Chem.* **1977**, *42*, 1249.
[152] K. Mislow, M. Raban, *Top. Stereochem.* **1967**, *1*, 1.
[153] S. Allenmark, *Chirality* **2003**, *15*, 409.
[154] T. Bürgi, A. Vargas, A. Baiker, *J. Chem. Soc. Perkin Trans. 2* **2002**, 1596.
[155] M. Losada, Y. J. Xu, *Phys. Chem. Chem. Phys.* **2007**, *9*, 3127.
[156] D. Cavagnat, L. Lespade, T. Buffeteau, *J. Phys. Chem. A* **2007**, *111*, 7014.
[157] G. Tarczay, G. Magyarfalvi, E. Vass, *Angew. Chem.* **2006**, *118*, 1807; *Angew. Chem. Int. Ed.* **2006**, *45*, 1775.
[158] G. W. Coates, *Chem. Rev.* **2000**, *100*, 1223.
[159] K. Maeda, E. Yashima, *Top. Curr. Chem.* **2006**, *265*, 47.
[160] N. Borho, Y. Xu, *Phys. Chem. Chem. Phys.* **2007**, *9*, 4514.
[161] A. Maeda, F. C. De Lucia, E. Herbst, J. C. Pearson, J. Riccobono, E. Trosell, R. K. Bohn, *Astrophys. J. Suppl. Ser.* **2006**, *162*, 428.
[162] T. N. Wassermann, P. Zielke, J. J. Lee, C. Cézard, M. A. Suhm, *J. Phys. Chem. A* **2007**, *111*, 7437.
[163] C. L. Lugez, F. J. Lovas, J. T. Hougen, N. Ohashi, *J. Mol. Spectrosc.* **1999**, *194*, 95.
[164] M. V. Vener, J. Sauer, *J. Chem. Phys.* **2001**, *114*, 2623.
[165] T. Scharge, C. Emmeluth, T. Häber, M. A. Suhm, *J. Mol. Struct.* **2006**, *786*, 86.
[166] E. Gloaguen, F. Pagliarulo, V. Brenner, W. Chin, F. Piuzzi, B. Tardivel, M. Mons, *Phys. Chem. Chem. Phys.* **2007**, *9*, 4491.
[167] V. Brenner, F. Piuzzi, I. Dimicoli, B. Tardivel, M. Mons, *Angew. Chem.* **2007**, *119*, 2515; *Angew. Chem. Int. Ed.* **2007**, *46*, 2463.
[168] A. G. Abo-Riziq, J. E. Bushnell, B. Crews, M. P. Callahan, L. Grace, M. S. de Vries, *Int. J. Quantum Chem.* **2005**, *105*, 437.
[169] K. Hatada, T. Kitayama, *Polym. Int.* **2000**, *49*, 11.
[170] J. Kumaki, T. Kawauchi, K. Okoshi, H. Kusanagi, E. Yashima, *Angew. Chem.* **2007**, *119*, 5444; *Angew. Chem. Int. Ed.* **2007**, *46*, 5348.
[171] H. D. Flack, *Helv. Chim. Acta* **2003**, *86*, 905.
[172] C. Frondel, *Am. Mineral.* **1978**, *63*, 17.
[173] M. Quack, *Angew. Chem.* **1989**, *101*, 588; *Angew. Chem. Int. Ed. Engl.* **1989**, *28*, 571.
[174] I. Weissbuch, L. Leiserowitz, M. Lahav, *Top. Curr. Chem.* **2005**, *259*, 123.
[175] K. H. Ernst, *Top. Curr. Chem.* **2006**, *265*, 209.
[176] G. Tomba, M. Lingenfelder, G. Costantini, K. Kern, F. Klappenberger, J. V. Barth, L. C. Ciacchi, A. De Vita, *J. Phys. Chem. A* **2007**, *111*, 12740.
[177] K. Soai, S. Osanai, K. Kadowaki, S. Yonekubo, T. Shibata, I. Sato, *J. Am. Chem. Soc.* **1999**, *121*, 11235.
[178] K. Soai, I. Sato, *Chirality* **2002**, *14*, 548.
[179] C. Viedma, *Phys. Rev. Lett.* **2005**, *94*, 065504.
[180] T. A. Beu, U. Buck, *Z. Phys. Chem.* **2000**, *214*, 437.
[181] I. Alkorta, J. Elguero, *J. Chem. Phys.* **2002**, *117*, 6463.
[182] B. Fehrensen, D. Luckhaus, M. Quack, *Chem. Phys.* **2007**, *338*, 90.
[183] A. Engdahl, B. Nelander, G. Karlstrom, *J. Phys. Chem. A* **2001**, *105*, 8393.
[184] I. Alkorta, K. Zborowski, J. Elguero, *Chem. Phys. Lett.* **2006**, *427*, 289.
[185] M. Elango, R. Parthasarathi, V. Subramanian, C. N. Ramachandran, N. Sathyamurthy, *J. Phys. Chem. A* **2006**, *110*, 6294.
[186] C. R. Quade, *J. Mol. Spectrosc.* **2000**, *203*, 200.
[187] J. P. I. Hearn, R. V. Cobley, B. J. Howard, *J. Chem. Phys.* **2005**, *123*, 134324.
[188] V. Dyczmons, *J. Phys. Chem. A* **2004**, *108*, 2080.
[189] M. Ehbrecht, F. Huisken, *J. Phys. Chem. A* **1997**, *101*, 7768.
[190] S. Coussan, M. E. Alikhani, J. P. Perchard, W. Q. Zheng, *J. Phys. Chem. A* **2000**, *104*, 5475.
[191] L. González, O. Mó, M. Yáñez, *J. Chem. Phys.* **1999**, *111*, 3855.
[192] R. A. Provencal, R. N. Casaes, K. Roth, J. B. Paul, C. N. Chapo, R. J. Saykally, G. S. Tschumper, H. F. Schaefer III, *J. Phys. Chem. A* **2000**, *104*, 1423.
[193] P. G. Jönsson, *Acta Crystallogr. Sect. B* **1976**, *32*, 232.
[194] D. Green, S. Hammond, J. Keske, B. H. Pate, *J. Chem. Phys.* **1999**, *110*, 1979.
[195] L. H. Xu, G. T. Fraser, F. J. Lovas, R. D. Suenram, C. W. Gillies, H. E. Warner, J. Z. Gillies, *J. Chem. Phys.* **1995**, *103*, 9541.
[196] T. Scharge, T. Häber, M. A. Suhm, *Phys. Chem. Chem. Phys.* **2006**, *8*, 4664.
[197] T. Scharge, C. Cézard, P. Zielke, A. Schütz, C. Emmeluth, M. A. Suhm, *Phys. Chem. Chem. Phys.* **2007**, *9*, 4472.
[198] I. Bako, T. Radnai, M. C. Bellisent-Funel, *J. Chem. Phys.* **2004**, *121*, 12472.
[199] A. Berkessel, J. A. Adrio, *J. Am. Chem. Soc.* **2006**, *128*, 13412.
[200] M. Buck, *Q. Rev. Biophys.* **1998**, *31*, 297.
[201] V. A. Soloshonok, *Angew. Chem.* **2006**, *118*, 780; *Angew. Chem. Int. Ed.* **2006**, *45*, 766.
[202] L. L. Thomas, T. J. Christakis, W. L. Jorgensen, *J. Phys. Chem. B* **2006**, *110*, 21198.
[203] R. Balabin, T. N. Wassermann, M. A. Suhm, unpublished results.
[204] R. F. Schaufele, T. Shimanouchi, *J. Chem. Phys.* **1967**, *47*, 3605.
[205] G. Solladie, R. G. Zimmermann, *Angew. Chem.* **1984**, *96*, 335; *Angew. Chem. Int. Ed. Engl.* **1984**, *23*, 348; H. G. Kuball, H. Brüning, *Chirality* **1997**, *9*, 407.
[206] R. R. Julian, S. Myung, D. E. Clemmer, *J. Am. Chem. Soc.* **2004**, *126*, 4110.
[207] D. Hermsdorf, S. Jauer, R. Signorell, *Mol. Phys.* **2007**, *105*, 951.
[208] F. Piuzzi, I. Dimicoli, M. Mons, B. Tardivel, Q. Zhao, *Chem. Phys. Lett.* **2000**, *320*.
[209] A. Abo-Riziq, B. O. Crews, M. P. Callahan, L. Grace, M. S. de Vries, *Angew. Chem.* **2006**, *118*, 5290; *Angew. Chem. Int. Ed.* **2006**, *45*, 5166.
[210] H. Fricke, A. Gerlach, M. Gerhards, *Phys. Chem. Chem. Phys.* **2006**, *8*, 1660.
[211] L. C. Snoek, T. van Mourik, P. Carcabal, J. P. Simons, *Phys. Chem. Chem. Phys.* **2003**, *5*, 4519.
[212] A. Gerlach, C. Unterberg, H. Fricke, M. Gerhards, *Mol. Phys.* **2005**, *103*, 1521.
[213] M. Quack in *Proc. of the 7th WATOC Congress* (Eds.: K. J. Naidoo, J. Brady, M. J. Field, J. Gao, M. Hann), Royal Society of Chemistry, Cambridge, **2006**, p. 3.

  